



ARTICLE

## Computational Analysis of Novel Extended Lindley Progressively Censored Data

Refah Alotaibi<sup>1</sup>, Mazen Nassar<sup>2,3</sup> and Ahmed Elshahhat<sup>4,\*</sup>

<sup>1</sup>Department of Mathematical Sciences, College of Science, Princess Nourah bint Abdulrahman University, P.O. Box 84428, Riyadh, 11671, Saudi Arabia

<sup>2</sup>Department of Statistics, Faculty of Science, King Abdulaziz University, Jeddah, 21589, Saudi Arabia

<sup>3</sup>Department of Statistics, Faculty of Commerce, Zagazig University, Zagazig, Egypt

<sup>4</sup>Faculty of Technology and Development, Zagazig University, Zagazig, 44519, Egypt

\*Corresponding Author: Ahmed Elshahhat. Email: aelshahhat@ftd.zu.edu.eg

Received: 13 April 2023 Accepted: 07 September 2023 Published: 15 December 2023

### ABSTRACT

A novel extended Lindley lifetime model that exhibits unimodal or decreasing density shapes as well as increasing, bathtub or unimodal-then-bathtub failure rates, named the Marshall-Olkin-Lindley (MOL) model is studied. In this research, using a progressive Type-II censored, various inferences of the MOL model parameters of life are introduced. Utilizing the maximum likelihood method as a classical approach, the estimators of the model parameters and various reliability measures are investigated. Against both symmetric and asymmetric loss functions, the Bayesian estimates are obtained using the Markov Chain Monte Carlo (MCMC) technique with the assumption of independent gamma priors. From the Fisher information data and the simulated Markovian chains, the approximate asymptotic interval and the highest posterior density interval, respectively, of each unknown parameter are calculated. Via an extensive simulated study, the usefulness of the various suggested strategies is assessed with respect to some evaluation metrics such as mean squared errors, mean relative absolute biases, average confidence lengths, and coverage percentages. Comparing the Bayesian estimations based on the asymmetric loss function to the traditional technique or the symmetric loss function-based Bayesian estimations, the analysis demonstrates that asymmetric loss function-based Bayesian estimations are preferred. Finally, two data sets, representing vinyl chloride and repairable mechanical equipment items, have been investigated to support the approaches proposed and show the superiority of the proposed model compared to the other fourteen lifetime models.

### KEYWORDS

Marshall-Olkin-Lindley model; reliability inference; Bayesian and classical inference; progressive Type-II censoring

### Abbreviations

ACI	Approximative confidence interval
ACL	Average confidence length
AIC	Akaike information criterion



APE	Alpha power exponential
Av.Es	Average estimates
BIC	Bayesian information criterion
BGR	Brooks-Gelman-Rubin
CA	Consistent Akaike
CP	Coverage percentage
E	Exponential
FP	Failure percentage
G	Gamma
GE	Generalized-exponential
GEnt	General entropy
HQ	Hannan-Quinn
HPD	Highest posterior density
HRF	Hazard rate function
KS	Kolmogorov-Smirnov
L	Lindley
M-H	Metropolis-Hastings
MCMC	Markov Chain Monte Carlo
MLE	Maximum likelihood estimator
MOAPE	Marshall-Olkin alpha power exponential
MOE	Marshall-Olkin exponential
MOG	Marshall-Olkin Gompertz
MOGE	Marshall-Olkin generalized exponential
MOL	Marshall-Olkin-Lindley
MOLE	Marshall-Olkin logistic-exponential
MONH	Marshall-Olkin Nadarajah-Haghighi
MOW	Marshall-Olkin Weibull
MRAB	Mean relative absolute bias
NH	Nadarajah-Haghighi
NL	Negative log-likelihood
PDF	Probability density function
PT-IIC	Progressive Type-II censored
QQ	Quantile-quantile
RF	Reliability function
RME	Repairable mechanical equipment
RMSE	Root mean squared-error
SE	Squared error
St.D	Standard deviation
St.E	Standard-error
W	Weibull

## 1 Introduction

One of the key research areas in the concept of distribution theory is the evolution of suggesting new statistical distributions. Such generalized distributions allow modelling for a range of disciplines, including reliability, engineering and medicine with even greater flexibility. The two-parameter Marshall-Olkin-Lindley (MOL) distribution suggested by Ghitany et al. [1] is one of the

novel versions of Marshall-Olkin models that take the conventional Lindley distribution as a baseline distribution. Assume that  $X$  is a lifetime random variable of an experimental item that follows the MOL distribution, denoted by  $MOL(\theta, \sigma)$ , with shape parameter  $\theta$  and scale parameter  $\sigma$ .

Hence, its probability density function (PDF),  $g(\cdot)$ , reliability function (RF),  $R(\cdot)$ , and hazard rate function (HRF),  $h(\cdot)$ , of  $x > 0$ , are given, respectively, by:

$$g(x; \theta, \sigma) = \frac{\theta \sigma^2 e^{-\sigma x} (x + 1)}{(\sigma + 1) \left[ 1 - \bar{\theta} e^{-\sigma x} \left( 1 + \frac{\sigma x}{\sigma + 1} \right) \right]^2}, \quad \theta, \sigma > 0, \tag{1}$$

$$R(x; \theta, \sigma) = \frac{\theta e^{-\sigma x} \left( 1 + \frac{\sigma x}{\sigma + 1} \right)}{1 - \bar{\theta} e^{-\sigma x} \left( 1 + \frac{\sigma x}{\sigma + 1} \right)} \tag{2}$$

and

$$h(x; \theta, \sigma) = \frac{\sigma^2 (x + 1)}{[\sigma (x + 1) + 1] \left[ 1 - \bar{\theta} e^{-\sigma x} \left( 1 + \frac{\sigma x}{\sigma + 1} \right) \right]}, \tag{3}$$

where  $\bar{\theta} = 1 - \theta$ . Obviously, the Lindley distribution can be obtained from (1) as a special case by setting  $\theta = 1$ . Using some specified values on the MOL's parameters of  $\theta$  and  $\sigma$ , via R 4.1.2 software, we plotted various shapes of the PDF and HRF of the MOL distribution, see Fig. 1. It shows that the density shapes are unimodal or decreasing while the HRF shapes are increasing, bathtub and unimodal then bathtub. Since these hazard rate shapes are quite beneficial in lifetime data modelling, hence the MOL distribution is justly flexible and can be considered to provide a good description of different plans of censored data, for details see Ghitany et al. [1]. A look at the literature reveals that just one study by do Espirito Santo et al. [2] used a complete sample to explore the estimations of the MOL distribution using six classical estimation approaches. On the other hand, no study considered the MOL distribution in the censoring case.

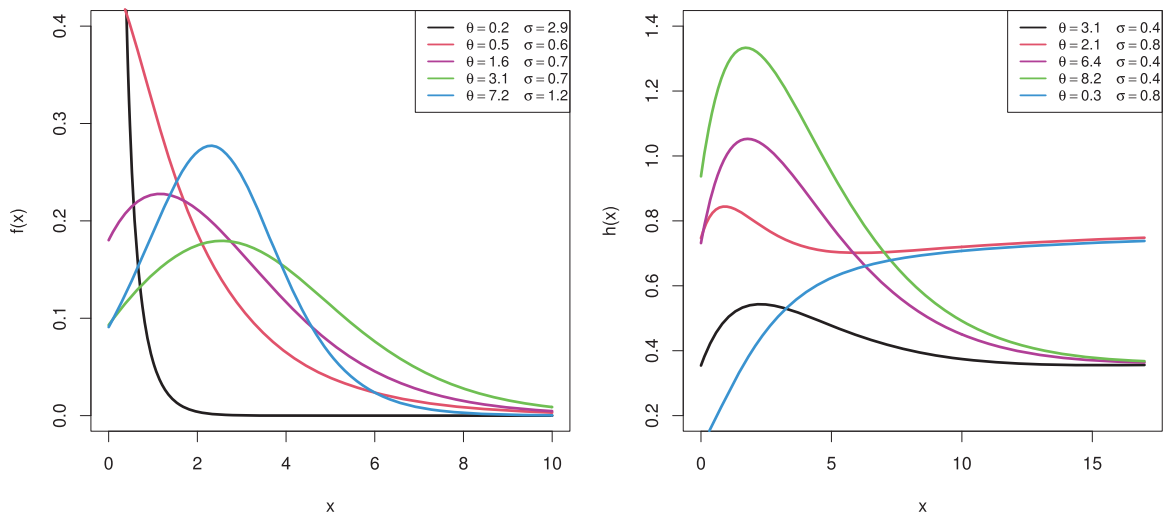


**Figure 1:** Various shapes for the density and hazard functions of MOEL distribution

Frequently, life testing studies are stopped before all of the components fail. Due to financial or time restrictions, it occurs. The observations that emerge from this type of scenario are known as the censored sample. The literature has developed a number of filtering techniques for the evaluation of various life-testing strategies. The two most popular censorship techniques among the various

techniques are Types I and II. The experimental units cannot be removed during a life-testing experiment, however, under any of these censorship techniques. This adaptability is featured in a life-testing experiment with progressive censoring. Since the publication of the book by Balakrishnan et al. [3], extensive research has been conducted on the various facets of progressive censoring. A recent book by Balakrishnan et al. [4] has an extensive compilation of different studies connected to the progressive censorship strategy.

In order to estimate the parameters of the MOL distribution, we work with the progressive Type-II censored (PT-IIC) sample in this study. The PT-IIC sample can be explained as follows: assume that a life testing experiment involving  $n$  units with a predetermined number progressive censoring scheme  $\mathbf{R} = (R_1, R_2, \dots, R_m)$ , where  $m < n$  is the desired number of observed failures. At the time of the first failure  $X_{1:m:n}$ , the experiment is stopped and  $R_1$  working units are removed. The experiment then resumes using the remaining  $n - 1 - R_1$  units, and when it reaches the second failure,  $X_{2:m:n}$ , it is stopped and  $R_2$  operating units are removed at random from the remaining  $n - 2 - R_1$  units, and so on. The experiment ends and all of the remaining units  $n - m - \sum_{i=1}^{m-1} R_i$  are eliminated when it reaches the  $m^{\text{th}}$  failure time  $X_{m:m:n}$ . The ordered observed failure times in this case are given by  $X_{1:m:n} < X_{2:m:n} < \dots < X_{m:m:n}$ , and the likelihood function for a PT-IIC sample can be expressed as:

$$L = A \prod_{i=1}^m g(x_{i:m:n}) [1 - G(x_{i:m:n})]^{R_i}, \quad (4)$$

where  $A$  is a constant that is independent of the parameters and  $G(x) = 1 - R(x)$ . For several practical lifetime models, a number of inferential techniques based on the PT-IIC scheme have been introduced. For instance, see Sultan et al. [5], Guo et al. [6], Joukar et al. [7], Elshahhat et al. [8], Alotaibi et al. [9], Okasha et al. [10] and Maiti et al. [11], as well as the references therein.

Due to the MOL distribution's flexibility and the PT-IIC scheme's effectiveness in gathering sample data, no study investigated the estimation problems of the MOL distribution in the case of the PT-IIC sample. Also, in the original work of Ghitany et al. [1], they just used the maximum likelihood approach to estimate the parameters of the MOL distribution without saying anything about the Bayesian estimation method. In addition, they estimated only the unknown parameters, while it is of interest to reliability engineers and other practitioners to see the performance of the reliability measures of the used distribution. Therefore, this paper's main goal is to examine frequentist and Bayesian inferences of the MOL distribution's unknown parameters under the PT-IIC, along with the related reliability indices, such as the RF and HRF. As expected, it is found that the maximum likelihood estimators (MLEs) of  $\theta$  and  $\sigma$  cannot be derived in closed form; instead, they must be obtained by simultaneously solving two non-linear equations. The MLEs of the RF and HRF are obtained using the invariance property. We suggest constructing the approximative confidence intervals (ACIs) for the various parameters, including RF and HRF, using the asymptotic distribution of the MLEs. We also take into account the Bayesian inference based on independent gamma priors and use two loss functions: squared error (SE) and general entropy (GEnt), which serve as symmetric and asymmetric loss functions, respectively. Due to the fact that the Bayesian estimators cannot be derived in closed form, we suggest using the Markov Chain Monte Carlo approach to get point estimates and the highest posterior density (HPD) credible intervals. The overall performance of the various techniques is compared using Monte Carlo simulations, and two data sets with various progressive censoring plans are examined for illustration.

The remainder of the article is structured as follows. We present the MLEs and ACIs of the unknown parameters, RF and HRF, in [Section 2](#). We acquire the Bayesian inference in [Section 3](#).

Sections 4 and 5 separately describe the findings of the Monte Carlo simulation and the analysis of two data sets, respectively. At last, we sum up the paper in Section 6.

## 2 Maximum Likelihood Estimation

In this part, we estimate the unknown parameters, RF and HRF of the MOL distribution using the method of maximum likelihood based on the PT-IIC sample. The ACIs of the different parameters are explained in addition to the point estimators. Assume that  $x_{1:m:n}, x_{2:m:n}, \dots, x_{m:m:n}$  is a PT-IIC sample of size  $m$  with progressive pattern  $R_1, \dots, R_m$  taken from the MOL population with PDF and RF as displayed in (1) and (2), respectively. Then the likelihood function, without the constant term, takes the following form based on (1) and (2), and (4):

$$L(\theta, \sigma) = \theta^n \sigma^{2m} (\sigma + 1)^m e^{-\sigma \sum_{i=1}^m (1+R_i)x_i} \prod_{i=1}^m \frac{(1 + \sigma y_i)^{R_i}}{[1 + \sigma - \bar{\theta} e^{-\sigma x_i} (1 + \sigma y_i)]^{2+R_i}}, \tag{5}$$

where  $x_i = x_{i:m:n}$  for simplicity and  $y_i = 1 + x_i$ . The log-likelihood function is expressed as follows, using Eq. (5):

$$\begin{aligned} \ell(\theta, \sigma) = & n \log(\theta) + 2m \log(\sigma) + m \log(\bar{\sigma}) - \sigma \sum_{i=1}^m (1 + R_i)x_i + \sum_{i=1}^m R_i \log(1 + \sigma y_i) \\ & - \sum_{i=1}^m (2 + R_i) \log[\bar{\sigma} - \bar{\theta} e^{-\sigma x_i} (1 + \sigma y_i)], \end{aligned} \tag{6}$$

where  $\bar{\sigma} = \sigma + 1$ . The likelihood equations are derived by calculating the first partial derivatives of (6) with regard to  $\theta$  and  $\sigma$  and equating each one to zero as shown below:

$$\frac{\partial \ell(\theta, \sigma)}{\partial \theta} = \frac{n}{\theta} - \sum_{i=1}^m \frac{(2 + R_i)e^{-\sigma x_i}(1 + \sigma y_i)}{\bar{\sigma} - \bar{\theta} e^{-\sigma x_i}(1 + \sigma y_i)} = 0 \tag{7}$$

and

$$\frac{\partial \ell(\theta, \sigma)}{\partial \sigma} = \frac{2m}{\sigma} + \frac{m}{\bar{\sigma}} - \sum_{i=1}^m (1 + R_i)x_i + \sum_{i=1}^m \frac{R_i y_i}{1 + \sigma y_i} - \sum_{i=1}^m \frac{(2 + R_i)\psi_i}{\bar{\sigma} - \bar{\theta} e^{-\sigma x_i}(1 + \sigma y_i)} = 0, \tag{8}$$

where  $\psi_i = 1 - \bar{\theta} e^{-\sigma x_i}[y_i - x_i(1 + \sigma y_i)]$ . It is obvious that analytical solutions to the likelihood equations in (7) and (8) in order to obtain the MLEs of  $\theta$  and  $\sigma$ , denoted by  $\hat{\theta}$  and  $\hat{\sigma}$ , are not possible. Therefore, to obtain the needed MLEs, any iteration process may be used, including the Newton-Raphson procedure. The MLEs of RF and HRF at a given time  $t$  can then be calculated using the invariance property of MLEs once the MLEs  $\hat{\theta}$  and  $\hat{\sigma}$  have been obtained. The MLEs of  $G(t)$  and  $h(t)$  in this instance are derived from (2) and (3) as follows:

$$\hat{R}(t) = \frac{\hat{\theta} e^{-\hat{\sigma} t} (1 + \frac{\hat{\sigma} t}{\hat{\sigma} + 1})}{1 - \hat{\theta} e^{-\hat{\sigma} t} (1 + \frac{\hat{\sigma} t}{\hat{\sigma} + 1})}$$

and

$$\hat{h}(t) = \frac{\hat{\sigma}^2 (t + 1)}{[\hat{\sigma} (t + 1) + 1] \left[ 1 - \hat{\theta} e^{-\hat{\sigma} t} (1 + \frac{\hat{\sigma} t}{\hat{\sigma} + 1}) \right]}.$$

Utilizing the asymptotic normality of the MLEs is the most common approach for establishing confidence bounds for the parameters. The MLEs' asymptotic distribution can be expressed as  $(\hat{\theta}, \hat{\sigma}) \sim N[(\theta, \sigma), \mathbf{J}^{-1}(\theta, \sigma)]$ , where  $\mathbf{J}^{-1}(\theta, \sigma)$  stands for the variance-covariance matrix obtained based on the Fisher information matrix denoted by  $\mathbf{J}$ . In practice, we use  $\mathbf{J}^{-1}(\hat{\theta}, \hat{\sigma})$  to estimate  $\mathbf{J}^{-1}(\theta, \sigma)$  due to the challenging second derivative expressions. In this case, we can write  $\mathbf{J}^{-1}(\hat{\theta}, \hat{\sigma})$  as follows:

$$\mathbf{J}^{-1}(\hat{\theta}, \hat{\sigma}) = \left( \begin{array}{cc} -\frac{\partial^2 \ell(\theta, \sigma)}{\partial \theta^2} & -\frac{\partial^2 \ell(\theta, \sigma)}{\partial \theta \partial \sigma} \\ -\frac{\partial^2 \ell(\theta, \sigma)}{\partial \sigma \partial \theta} & -\frac{\partial^2 \ell(\theta, \sigma)}{\partial \sigma^2} \end{array} \right)_{(\theta, \sigma) = (\hat{\theta}, \hat{\sigma})}^{-1} = \begin{pmatrix} \widehat{\text{var}}(\hat{\theta}) & \widehat{\text{cov}}(\hat{\theta}, \hat{\sigma}) \\ \widehat{\text{cov}}(\hat{\sigma}, \hat{\theta}) & \widehat{\text{var}}(\hat{\sigma}) \end{pmatrix}, \quad (9)$$

with

$$\begin{aligned} \frac{\partial^2 \ell(\theta, \sigma)}{\partial \theta^2} &= -\frac{n}{\theta^2} - \sum_{i=1}^m \frac{(2 + R_i) e^{-2\sigma x_i} (1 + \sigma y_i)^2}{\phi_i^2}, \\ \frac{\partial^2 \ell(\theta, \sigma)}{\partial \sigma^2} &= -\frac{2m}{\sigma^2} - \frac{m}{\bar{\sigma}^2} + \sum_{i=1}^m \frac{R_i y_i^2}{(1 + \sigma y_i)^2} - \sum_{i=1}^m \frac{(2 + R_i) \varpi_i}{\phi_i} - \sum_{i=1}^m \frac{(2 + R_i) \psi_i^2}{\phi_i^2} \end{aligned}$$

and

$$\frac{\partial^2 \ell(\theta, \sigma)}{\partial \theta \partial \sigma} = \sum_{i=1}^m \frac{(2 + R_i) \psi_i}{\phi_i} - \sum_{i=1}^m \frac{(2 + R_i) e^{-\sigma x_i} (1 + \sigma y_i) \psi_i}{\phi_i^2},$$

where  $\phi_i = \bar{\sigma} - \bar{\theta} e^{-\sigma x_i} (1 + \sigma y_i)$  and  $\varpi_i = x_i \bar{\theta} e^{-\sigma x_i} [x_i (1 + \sigma y_i) - 2y_i]$  and  $\psi_i = e^{-\sigma x_i} [y_i - x_i (1 + \sigma y_i)]$ . Then, the  $100(1 - \alpha)\%$  ACIs of  $\theta$  and  $\sigma$  can be computed, respectively, as:

$$\hat{\theta} \pm z_{\alpha/2} \sqrt{\widehat{\text{var}}(\hat{\theta})}, \text{ and } \hat{\sigma} \pm z_{\alpha/2} \sqrt{\widehat{\text{var}}(\hat{\sigma})},$$

where  $\widehat{\text{var}}(\hat{\theta})$  and  $\widehat{\text{var}}(\hat{\sigma})$  are the main diagonal elements of (9), respectively, and  $z_{\alpha/2}$  is the upper  $(\alpha/2)^{\text{th}}$  percentile point of the standard normal distribution. On the other hand, we must first determine the variances of respective estimators for the RF and HRF in order to construct such intervals. Here, we approximate these variances using the delta approach. The following derivatives obtained from (2) and (3), respectively, are required in order to use the delta method:

$$\begin{aligned} R_\theta &= \frac{\partial R(t; \theta, \sigma)}{\partial \theta} = \frac{G(t; \theta, \sigma)}{\theta} [1 - R(t; \theta, \sigma)], \\ R_\sigma &= \frac{\partial R(t; \theta, \sigma)}{\partial \sigma} = \frac{\theta t e^{-\sigma t}}{\bar{\sigma} \phi_t} - \frac{\bar{\theta} t \sigma R(t; \theta, \sigma) e^{-\sigma t} (1 + \bar{\sigma} y_t)}{\bar{\sigma}^2 \phi_t} - t R(t; \theta, \sigma), \\ h_\theta &= \frac{\partial h(t; \theta, \sigma)}{\partial \theta} = -\frac{h(t; \theta, \sigma) e^{-\sigma t} (1 + \sigma y_t)}{\phi_t \bar{\sigma}} \end{aligned}$$

and

$$h_\sigma = \frac{\partial h(t; \theta, \sigma)}{\partial \sigma} = \frac{\sigma y_t}{\phi_t (1 + \sigma y_t)} \left[ 2 - \frac{\sigma y_t}{(1 + \sigma y_t)} \right] - \frac{\bar{\theta} t \sigma h(t; \theta, \sigma) e^{-\sigma t} (1 + \bar{\sigma} y_t)}{\bar{\sigma}^2 \phi_t},$$

where  $\phi_t = \bar{\sigma} - \bar{\theta} e^{-\sigma t} (1 + \sigma (1 + t))$  and  $y_t = 1 + t$ .

Suppose that  $\Delta_R = (R_\theta, R_\sigma)|_{(\theta, \sigma) = (\hat{\theta}, \hat{\sigma})}$  and  $\Delta_h = (h_\theta, h_\sigma)|_{(\theta, \sigma) = (\hat{\theta}, \hat{\sigma})}$ , then we can obtain the approximated estimated variances of  $\hat{R}(t)$  and  $\hat{h}(t)$ , respectively, as follows:

$$\widehat{\text{var}}(\hat{R}) \approx [\Delta_R \mathbf{J}^{-1}(\hat{\theta}, \hat{\sigma}) \Delta_R^\top] \text{ and } \widehat{\text{var}}(\hat{h}) \approx [\Delta_h \mathbf{J}^{-1}(\hat{\theta}, \hat{\sigma}) \Delta_h^\top],$$

As a result, with  $100(1-\alpha)\%$  confidence level, the ACIs that align to  $G(t)$  and  $h(t)$  can be acquired, respectively, as follows:

$$\hat{R}(t) \pm z_{\alpha/2} \sqrt{\widehat{\text{var}}(\hat{R})}, \text{ and } \hat{h}(t) \pm z_{\alpha/2} \sqrt{\widehat{\text{var}}(\hat{h})}.$$

### 3 Bayesian Estimation

For analyzing failure time data, the Bayesian estimation approach has attracted a lot of attention. It uses one's past knowledge of the parameters and also takes into account the information that is readily available. In this section, the Bayesian estimators of  $\theta, \sigma, R(t)$  and  $h(t)$  are considered under the assumption that the two unknown parameters are independent and have gamma prior distributions. We consider the use of independent gamma priors due to the flexibility of gamma distribution and to avoid adding more complexity to the posterior distribution. Moreover, independent priors are considered because they are rather straightforward and concise, which may not produce many challenging computational and inferential problems. Despite dependent priors appearing more appealing in some practical contexts, the dependent property between parameters cannot be justified subjectively based on historical data and expert knowledge where such prior information may be extremely rare. Hence, for the sake of simplicity, independent priors are more widely used in statistics under the Bayesian method. In order to get the Bayesian estimators, two loss functions are offered to get the point estimators, namely SE and GEnt loss functions. Besides acquiring the point estimators, the HPD credible intervals are also obtained. Suppose that  $\theta \sim G(a_1, b_1)$  and  $\sigma \sim G(a_2, b_2)$ , where  $a_j, b_j, j = 1, 2$  are the hyper-parameters. Therefore, the joint prior of  $\theta$  and  $\sigma$  can be expressed as shown below:

$$q(\theta, \sigma) \propto \theta^{a_1-1} \sigma^{a_2-1} e^{-(b_1\theta+b_2\sigma)}, \theta, \sigma > 0. \tag{10}$$

The posterior distribution of the unknown parameters  $\theta$  and  $\sigma$  can be obtained by combining the likelihood function in (5) with the joint prior distribution provided (10) and by applying the Bayes theorem as follows:

$$g(\theta, \sigma | \underline{x}) = \frac{\theta^{n+a_1-1} \sigma^{2m+a_2-1} \bar{\sigma}^m e^{-\sigma [\sum_{i=1}^m (1+R_i)x_i + b_2]} - b_1 \theta}{C} \prod_{i=1}^m \frac{(1 + \sigma y_i)^{R_i}}{[\bar{\sigma} - \bar{\theta} e^{-\sigma x_i} (1 + \sigma y_i)]^{2+R_i}}, \tag{11}$$

where  $\underline{x} = (x_1, \dots, x_m)$  and  $C$  is the normalized constant.

If one setting  $a_j = b_j = 0$  for  $j = 1, 2$  in (10), the joint posterior density (11) will then be in proportion to the likelihood function (5), i.e.,  $g(\theta, \sigma | \underline{x}) \propto (\theta\sigma)^{-1} L(\theta, \sigma)$ , which is the non-informative case. From a Bayesian viewpoint, there is clearly no way in which one can say that one prior is better than any other. Generally, if the proper prior information is available, it is better to use the informative prior(s) than the non-informative prior(s). Otherwise, if one does not have sufficient prior information, it is better to use a non-informative prior distribution. Since the Bayesian estimates using SE loss function with non-informative priors behave like the maximum likelihood estimates whereas those with informative priors behave much better than others, it is always better to use the frequentist estimates rather than the Bayesian estimates because the latter are computationally more expensive when the MCMC procedure is used. In Section 4, to evaluate the sensitivity of the priors, some discussions about various sets of prior distributions are reported.

Now, in order to derive the Bayesian estimators, we take into account the SE and GEnt loss functions. The Bayesian estimator for the SE loss function is the posterior mean, which considers overestimation and underestimation equally. In contrast hand, the GEnt loss function offers different

influences for overestimation and underestimation. Calabria et al. [12] introduced the GEnt loss function, which is defined as:

$$GEnt(\tilde{\lambda}, \lambda) \propto \left(\frac{\tilde{\lambda}}{\lambda}\right)^{\mu} - \mu \log\left(\frac{\tilde{\lambda}}{\lambda}\right) - 1,$$

where  $\mu$  is a parameter that controls the level of asymmetry and  $\tilde{\lambda}$  is the Bayesian estimator of  $\lambda$ . Below is the Bayesian estimator of  $\lambda$  using the GEnt loss function:

$$\tilde{\lambda}_{GEnt} = [E_{\lambda}(\lambda^{-\mu})]^{-\frac{1}{\mu}}, \quad (12)$$

given that  $E_{\delta}(\delta^{-\kappa})$  exists and is finite. Assume that  $\vartheta(\theta, \sigma)$  is a function of the unknown parameters, we may easily derive its Bayesian estimator using SE and GEnt loss functions, respectively, as follows:

$$\tilde{\vartheta}_{SE}(\theta, \sigma) = \int_0^{\infty} \int_0^{\infty} \vartheta(\theta, \sigma) g(\theta, \sigma | \underline{x}) d\theta d\sigma \quad (13)$$

and

$$\tilde{\vartheta}_{GEnt}(\theta, \sigma) = \left[ \int_0^{\infty} \int_0^{\infty} [\vartheta(\theta, \sigma)]^{-\mu} g(\theta, \sigma | \underline{x}) d\theta d\sigma \right]^{-\frac{1}{\mu}} \quad (14)$$

It is obvious that it is difficult to determine the Bayesian estimators using (13) and (14) analytically. In order to acquire the Bayesian estimates of  $\theta$  and  $\sigma$  and the related HPD credible intervals, we suggest using the MCMC procedure. We must first determine the full conditional distributions of the unknown parameters from (11) as follows:

$$g(\theta | \sigma, \underline{x}) \propto \theta^{n+a_1-1} \exp \left\{ - \sum_{i=1}^m (2 + R_i) \log [\bar{\sigma} - \bar{\theta} e^{-\sigma x_i} (1 + \sigma y_i)] - b_1 \theta \right\} \quad (15)$$

and

$$g(\sigma | \theta, \underline{x}) \propto \sigma^{2m+a_2-1} \bar{\sigma}^m e^{-\sigma [\sum_{i=1}^m (1+R_i)x_i + b_2]} \prod_{i=1}^m \frac{(1 + \sigma y_i)^{R_i}}{[\bar{\sigma} - \bar{\theta} e^{-\sigma x_i} (1 + \sigma y_i)]^{2+R_i}}. \quad (16)$$

It is evident that the conditional distributions of  $\theta$  and  $\sigma$  as provided in (15) and (16) cannot be represented in standard forms, but their graphs are equivalent to the normal distribution. As a result, we employ the Metropolis-Hastings (M-H) algorithm with normal proposal distribution with asymptotic variances to produce random samples from these distributions. The steps that follow now demonstrate how to get the required samples.

**Step 1.** Set  $k = 1$ .

**Step 2.** Begin with the initial guesses  $(\theta^{(0)}, \sigma^{(0)}) = (\hat{\theta}, \hat{\sigma})$ .

**Step 3.** From (15), generate  $\theta^{(k)}$  using normal proposal distribution, i.e.,  $N(\theta^{(0)}, \widehat{var}(\theta^{(0)}))$ , by using the M-H steps, where  $\widehat{var}(\theta^{(0)}) \cong \widehat{var}(\hat{\theta})$  is given by (9).

**Step 4.** Use (16) to get  $\sigma^{(k)}$  using the M-H steps with normal proposal distribution, i.e.,  $N(\sigma^{(0)}, \widehat{var}(\sigma^{(0)}))$ , where  $\widehat{var}(\sigma^{(0)}) \cong \widehat{var}(\hat{\sigma})$  is given by (9).

**Step 5.** Based on the generated  $\theta^{(k)}$  and  $\sigma^{(k)}$ , obtain

$$R^{(k)}(t) = \frac{\theta^{(k)} e^{-\sigma^{(k)} t} (1 + \frac{\sigma^{(k)} t}{\sigma^{(k)} + 1})}{1 - \bar{\theta}^{(k)} e^{-\sigma^{(k)} t} (1 + \frac{\sigma^{(k)} t}{\sigma^{(k)} + 1})}$$

and

$$h^{(k)}(t) = \frac{\sigma^{2(k)}(t+1)}{[\sigma^{(k)}(t+1) + 1] \left[ 1 - \bar{\theta}^{(k)} e^{-\sigma^{(k)} t} (1 + \frac{\sigma^{(k)} t}{\sigma^{(k)} + 1}) \right]},$$

**Step 6.** Put  $k = k + 1$ .

**Step 7.** Repeat steps 3–6,  $M$  times to compute

$$[\beta^{(1)}, \dots, \beta^{(M)}],$$

where  $\beta = \theta, \sigma, R(t)$  or  $h(t)$ .

In this study, the first  $B$  generated samples are discarded in order to ensure convergence and remove the appeal of initial guesses. In this situation, we possess  $\beta^{(k)}, k = B + 1, \dots, M$ . The Bayesian estimate of  $\beta$  based on the SE and GEnt loss functions can be calculated using large  $M$ , respectively, as:

$$\tilde{\beta}_{SE} = \frac{1}{M - B} \sum_{k=B+1}^M \beta^{(k)} \quad \text{and} \quad \tilde{\beta}_{GEnt} = \left\{ \frac{1}{M - B} \sum_{k=B+1}^M [\beta^{(k)}]^{-\mu} \right\}^{-\frac{1}{\mu}}.$$

To construct the HPD credible intervals of  $\beta$ , order  $\beta^{(k)}, k = B + 1, \dots, M$ . Therefore, the  $100(1 - \alpha)\%$  HPD credible interval of  $\beta$  will be  $[\beta^{(k^*)}, \beta^{(k^* + (1-\alpha)(M-B))}]$ , where  $k^* = B + 1, B + 2, \dots, M$  is determined such that:

$$\beta^{(k^* + [(1-\alpha)(M-B)])} - \beta^{(k^*)} = \min_{1 \leq l \leq \alpha(M-B)} [\beta^{(l + [(1-\alpha)(M-B)])} - \beta^{(k^*)}],$$

where  $[v]$  stands for the biggest integer that is less than or equal to  $v$ .

#### 4 Monte Carlo Simulation

To evaluate the behavior of the proposed estimators of  $\theta, \sigma, R(t)$  and  $h(t)$  developed in the proceeding sections, Monte Carlo simulation experiments are conducted. For this target, we simulate 1,000 PT-IIC samples from MOL(0.8, 0.4) based on various choices of  $n, m$  and progressive pattern  $\mathbf{R}$ . Taking  $t = 0.2$ , the actual values of  $R(t)$  and  $h(t)$  are 0.970 and 0.104, respectively. Using  $n(=50, 90)$ , the proposed numerical experiments are performed by taking  $m$  as a failure percentage (FP) of each  $n$  as  $\frac{m}{n}(=40, 80)\%$ . Moreover, for each set of  $(n, m)$ , different progressive patterns  $\mathbf{R} = (R_1, R_2, \dots, R_m)$  are considered as:

Scheme-1 :  $\mathbf{R} = (n - m, 0^*(m - 1))$ ,

Scheme-2 :  $\mathbf{R} = (0^*(\frac{m}{2} - 1), n - m, 0^*(\frac{m}{2}))$ ,

Scheme-3 :  $\mathbf{R} = (0^*(m - 1), n - m)$ ,

where  $\mathbf{R} = (1, 0, 0, 0, 1)$  is denoted by  $\mathbf{R} = (1, 0^*3, 1)$  for short notation.

Once the 1,000 PT-IIC samples collected, the maximum likelihood and 95% ACI estimates of  $\theta$ ,  $\sigma$ ,  $R(t)$  and  $h(t)$  are calculated utilizing via 'maxLik' package (by Henningsen et al. [13]) in R 4.1.2 software. To develop the Bayesian MCMC inferences of the same unknown MOL parameters, by according to the mean and variance of the gamma density, two informative sets of the hyperparameters  $a_i$  and  $b_i$  for  $i = 1, 2$  of  $\theta$  and  $\sigma$  are used namely: prior-1:  $(a_1, a_2, b_1, b_2) = (4, 2, 5, 5)$  and prior-2:  $(a_1, a_2, b_1, b_2) = (8, 4, 10, 10)$ . Following Kundu [14] and Dey et al. [15], the given hyperparameter values of  $a_i, b_i, i = 1, 2$  of the unknown MOL parameters are chosen in such a way that the prior mean becomes the expected value of the corresponding parameter. Using the M-H algorithm sampler, from SE and GEnt (for  $\mu(= -2, +2)$ ) loss functions, the Bayesian point estimates of  $\theta, \sigma, R(t)$  and  $h(t)$  are calculated based on 12,000 MCMC samples after ignoring the first 2,000 variates as burn-in. Further, from 10,000 MCMC samples, the 95% HPD credible intervals of  $\theta, \sigma, R(t)$  or  $h(t)$  are calculated also. All Bayesian evaluations of the unknown parameters  $\theta$  and  $\sigma$  or the reliability time parameters  $R(t)$  and  $h(t)$  are performed via 'coda' package (by Plummer et al. [16]) in R 4.1.2 software. All necessary computational algorithms were performed on a laptop with Core(TM) i5-2410M processor and 4.00 GB of RAM. It is better to be noted, regarding the benefits of both 'maxLik' and 'coda' programming packages, that the CPU time required per iteration is not expensive.

To monitor whether the simulated Markovian sample is sufficiently close to the target posterior, beside the trace and autocorrelation plots, we purpose to consider the Brooks-Gelman-Rubin (BGR) diagnostic statistic, which evaluates the convergence by analyzing the difference between the variance-within chains and the variance-between chains for each model parameter, for details see [17]. To establish this purpose, by running two chains using  $n[\text{FP}\%] = 50[40\%]$ , Scheme-1, and prior-1 (as an example), we plotted the suggested convergence diagnostics in Figs. 2 and 3 via R 4.1.2 software. It is clear, from Fig. 2, that the MCMC iterations are converged well. On the other hand, Fig. 3 shows that the proposed BGR diagnoses close to one after simulating the first 2,000 iterations, which means that the combustion sample has an adequate size to ignore the influence of the initial guesses, and thus the simulated chains converged well.

The average estimates (Av.Es) from classical (or Bayesian) approach of  $\theta, \sigma, R(t)$  and  $h(t)$  (say  $\omega$ ) are given by:

$$\bar{\omega}_d = \frac{1}{1,000} \sum_{i=1}^{1,000} \check{\omega}_d^{(i)}, \quad d = 1, 2, 3, 4,$$

where  $\check{\omega}^{(i)}$  is the calculated estimate of  $\omega$  at the  $i$ th simulated sample,  $\omega_1 = \theta, \omega_2 = \sigma, \omega_3 = R(t)$  and  $\omega_4 = h(t)$ .

Further, the comparison between point estimates of  $\omega$  is made based on their root mean squared-errors (RMSEs) and mean relative absolute biases (MRABs) as:

$$\text{RMSE}(\check{\omega}_d) = \sqrt{\frac{1}{1000} \sum_{i=1}^{1000} (\check{\omega}_d^{(i)} - \omega_d)^2}, \quad d = 1, 2, 3, 4,$$

and

$$\text{MRAB}(\check{\omega}_d) = \frac{1}{1000} \sum_{i=1}^{1000} \frac{1}{\omega_d} |\check{\omega}_d^{(i)} - \omega_d|, \quad d = 1, 2, 3, 4,$$

respectively.

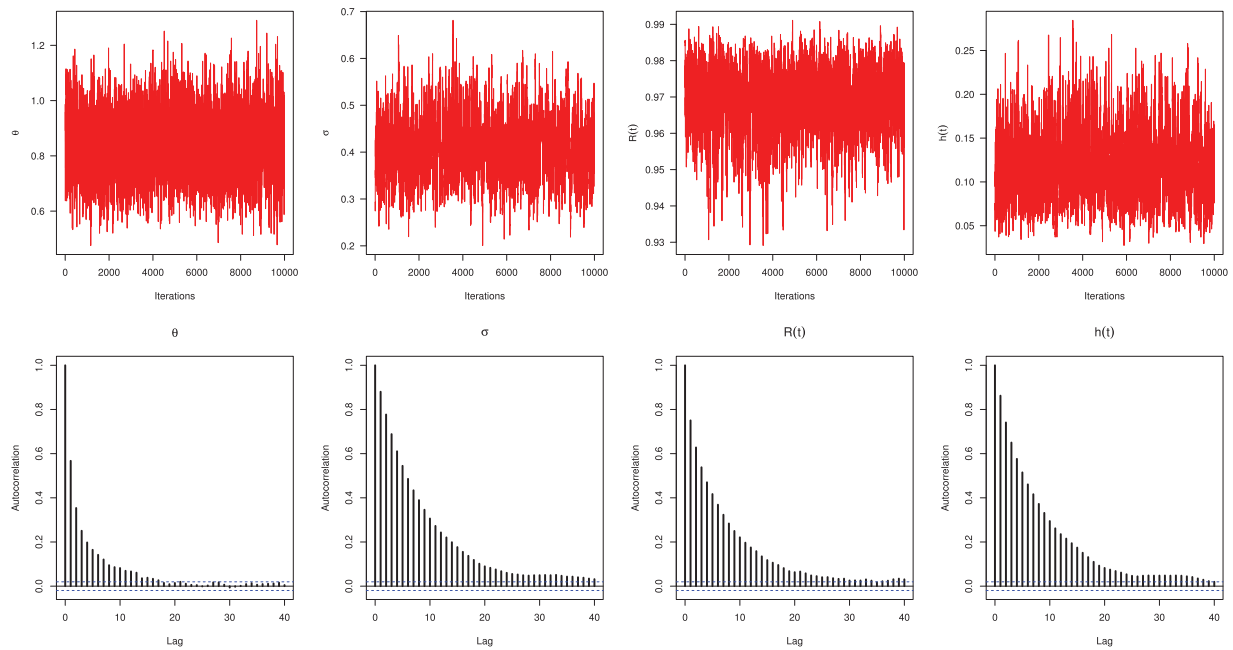


**Figure 2:** Trace (top) and Autocorrelation (bottom) plots for MCMC draws of  $\theta$ ,  $\sigma$ ,  $R(t)$  and  $h(t)$  in Monte Carlo simulation

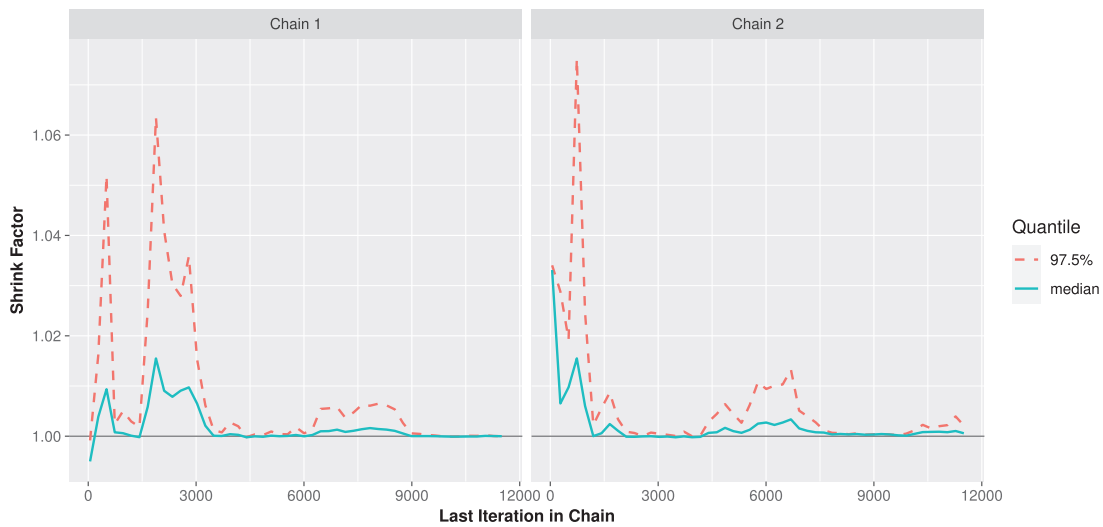


**Figure 3:** The BGR diagnostic for MCMC draws of  $\theta$  (left) and  $\sigma$  (right) in Monte Carlo simulation

Furthermore, the comparison between interval estimates of the same unknown parameters is made using their average confidence lengths (ACLs) and coverage percentages (CPs) which can be computed as

$$ACL_{(1-\alpha)\%}(\omega_d) = \frac{1}{1000} \sum_{i=1}^{1000} \left( \mathcal{U}_{\omega_d^{(i)}} - \mathcal{L}_{\omega_d^{(i)}} \right), \quad d = 1, 2, 3, 4,$$

and

$$CP_{(1-\alpha)\%}(\omega_d) = \frac{1}{1000} \sum_{i=1}^{1000} \mathbf{1}_{\left(\mathcal{L}_{\omega_d^{(i)}}; \mathcal{U}_{\omega_d^{(i)}}\right)}(\omega_d), \quad d = 1, 2, 3, 4,$$

respectively, where  $\mathbf{1}(\cdot)$  is the indicator function and  $\mathcal{L}(\cdot)$  and  $\mathcal{U}(\cdot)$  denote the lower and upper bounds, respectively, of  $(1 - \alpha)\%$  asymptotic (or HPD credible) interval of  $\omega_d$ .

Heatmap is a method of representing data graphically where values are depicted by color, making it easy to visualize complex data and understand it at a glance. So, via R data visualization, all numerical results of  $\theta$ ,  $\sigma$ ,  $R(t)$  and  $h(t)$  are displayed with heatmap plots in Figs. 4–7, respectively. Here, following the graphical tools reported in Elshahhat [18], the suggested heatmaps are plotted via R 4.1.2 software. Each heatmap range is classified from lowest to highest values with the colors cyan, red, and yellow, respectively. Each heatmap also displays the proposed estimation methods and the specified test settings on the “x-axis” and “y-axis” lines, respectively. In the supplementary file, all simulation tables of  $\theta$ ,  $\sigma$ ,  $R(t)$  and  $h(t)$  are listed. Furthermore, for specification, several notations of the estimation methods have been used in Figs. 4–7 such as (based on Prior 1 (say P1) as an example) the Bayesian estimates based on SE loss mentioned as “SE-P1” as well as the Bayesian estimates based on GEnt loss for  $\mu = -2$  and  $+2$  mentioned as “GE1-P1” and “GE2-P1”, respectively.

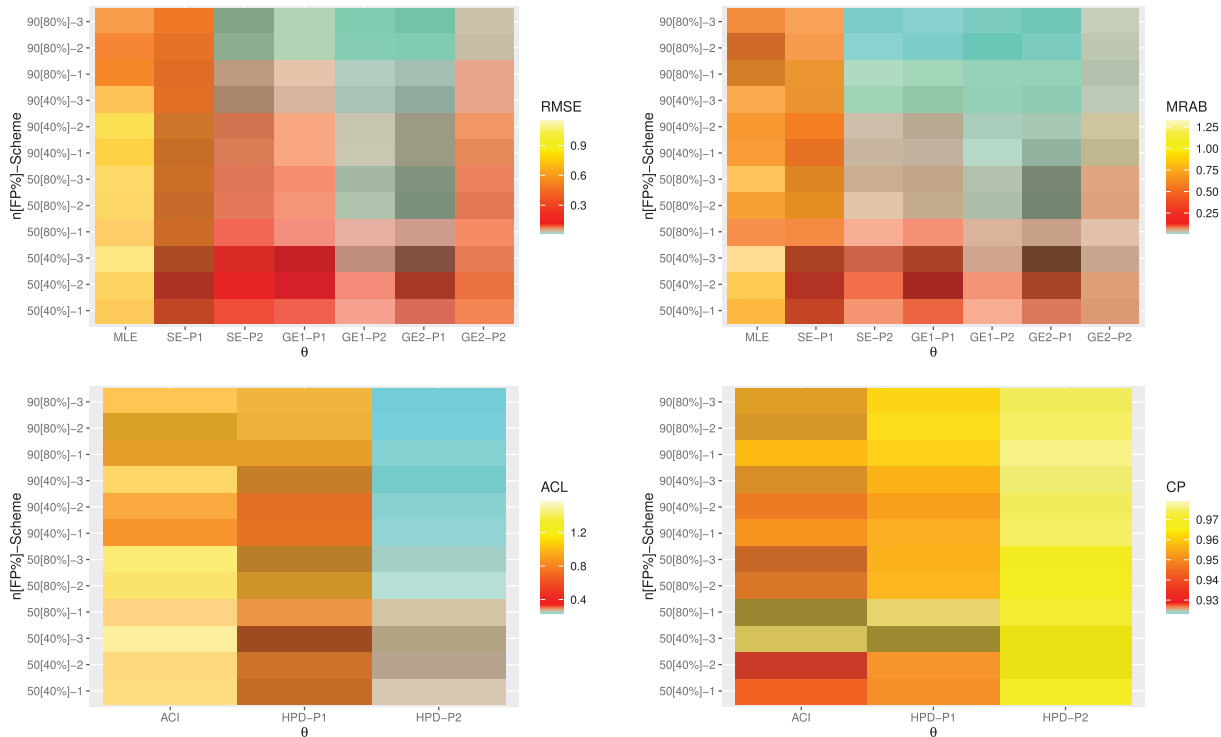


Figure 4: Heatmap plots for the point and interval results of  $\theta$

From Figs. 4–7, in terms of the lowest RMSE, MRAB and ACL values as well as the highest CP values, the following comments can be drawn:

- Generally, the proposed point and interval estimates of  $\theta$ ,  $\sigma$ ,  $R(t)$  and  $h(t)$  of the MOL model in presence of PT-IIC data behave satisfactorily.

- As  $n$ (or FP) increases, the maximum likelihood and Bayesian estimates of  $\theta$ ,  $\sigma$ ,  $R(t)$  and  $h(t)$  perform well. A similar observation is reached when  $n - m$  decreases.
- Bayesian estimates against the GEnt loss function perform superior than those obtained against the SE loss function, and both perform better compared to the other estimates due to the gamma prior information. Similar result is also observed in the case of HPD credible interval estimates.
- To evaluate the effect of parameter loss, it can be seen that the asymmetric Bayes estimates of  $\theta$ ,  $\sigma$ ,  $R(t)$  or  $h(t)$  are overestimates (or underestimates) for  $\mu < 0$  (or  $\mu > 0$ ). This is one of the useful properties of working with the GEnt loss function.
- Comparing the considered prior sets 1 and 2, due to the variance of prior 2 is smaller than the variance of prior 1, it is observed that the Bayesian estimates and associated HPD credible intervals under prior 2 of all unknown parameters have good perform than others.
- Asymmetric Bayesian estimates of  $\theta$ ,  $\sigma$ ,  $R(t)$  or  $h(t)$  have overestimates (when  $(\mu < 0)$ ) and underestimates (when  $(\mu > 0)$ ).
- Comparing the censoring schemes 1, 2 and 3, it is clear that the both proposed point and interval estimates of  $\theta$  and  $h(t)$  perform better using scheme-1 (when the survived items  $n - m$  drawn at  $x_1$ ); of  $R(t)$  perform better using scheme-3 (when the survived items  $n - m$  drawn at  $x_m$ ); and of  $\sigma$  perform better based on scheme-1 (for likelihood inference) while based on scheme-3 (for Bayesian inference).
- Finally, to estimate the MOL distribution parameters or its reliability characteristics under PT-IIC mechanism, the Bayesian M-H algorithm method is recommended.

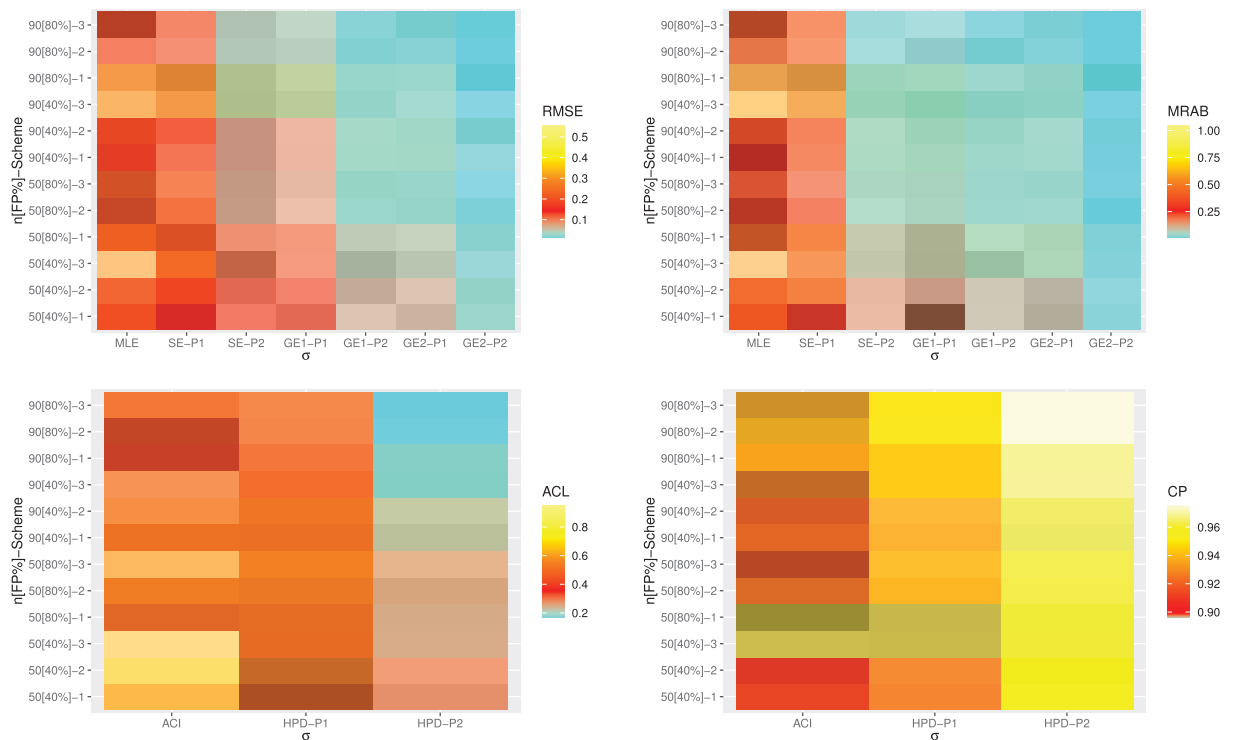
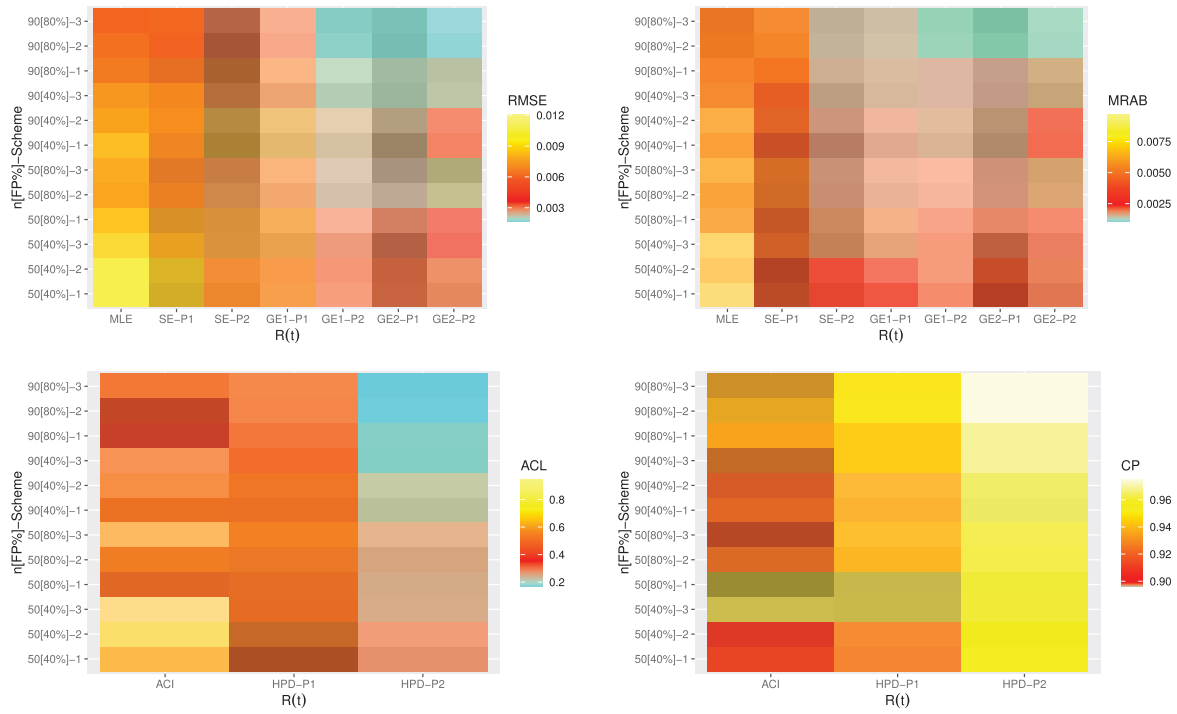
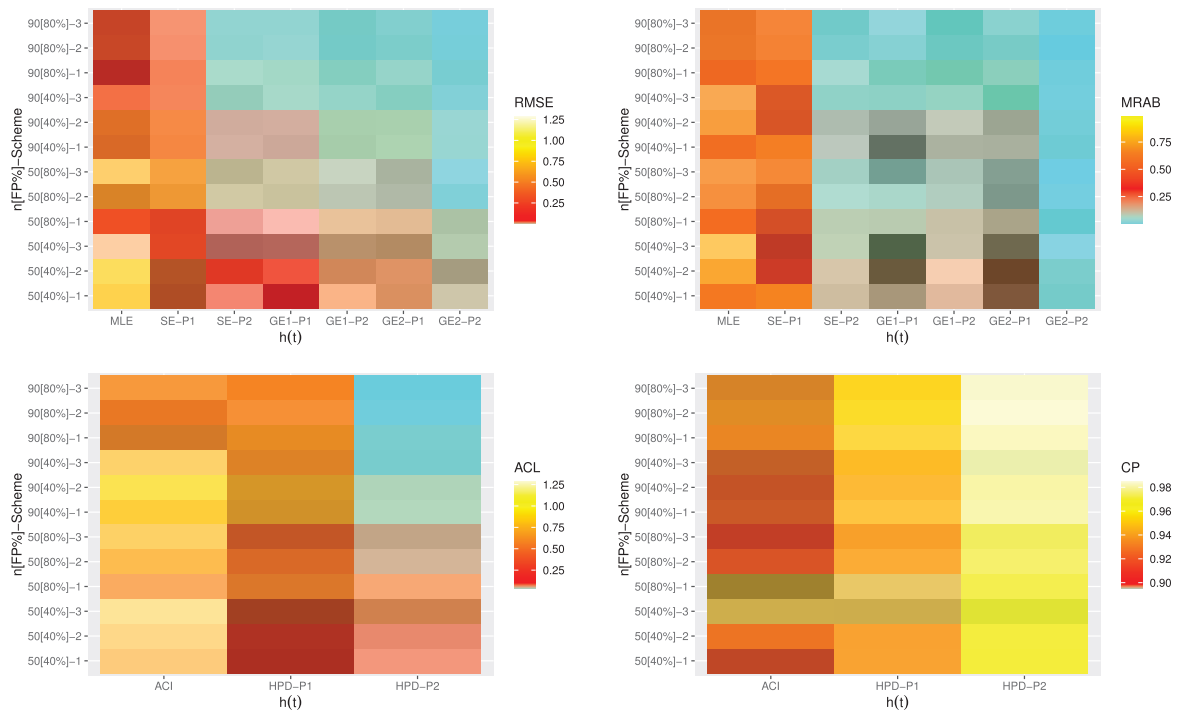


Figure 5: Heatmap plots for the point and interval results of  $\sigma$



**Figure 6:** Heatmap plots for the point and interval results of  $R(t)$



**Figure 7:** Heatmap plots for the point and interval results of  $h(t)$

## 5 Real-Life Applications

In order to demonstrate the significance of the suggested inferential methodologies and the applicability of study objectives to actual phenomena, this part presents two practical applications from the domains of engineering and chemistry.

### 5.1 Vinyl Chloride

Vinyl chloride is a known human carcinogen and a rapidly burning colorless gas. In this application, 34 data points (measured in milligrams/liter) as presented in see [Table 1](#) for vinyl chloride were taken from clean-up-gradient monitoring wells and analyzed. This data set was reported by Bhaumik et al. [19] and re-analyzed also by Elshahhat et al. [20], Alotaibi et al. [21], Elshahhat et al. [22].

**Table 1:** Data points of vinyl chloride

0.1	0.1	0.2	0.2	0.4	0.4	0.4	0.5	0.5	0.5	0.6	0.6
0.8	0.9	0.9	1.0	1.1	1.2	1.2	1.3	1.8	2.0	2.0	2.3
2.4	2.5	2.7	2.9	3.2	4.0	5.1	5.3	6.8	8.0		

To verify the flexibility of the MOL model, the MOL distribution is compared with fourteen well-known distributions, (for  $x > 0$  and  $\alpha, \theta, \sigma$ ), namely; Marshall-Olkin exponential (MOE( $\theta, \sigma$ )) by Marshall et al. [23], Marshall-Olkin Weibull (MOW( $\alpha, \theta, \sigma$ )) by Cordeiro et al. [24], Marshall-Olkin Gompertz (MOG( $\alpha, \theta, \sigma$ )) by Eghwerido et al. [25], Marshall-Olkin generalized exponential (MOGE( $\alpha, \theta, \sigma$ )) by Ristić et al. [26], Marshall-Olkin logistic-exponential (MOLE( $\alpha, \theta, \sigma$ )) by Mansoor et al. [27], Marshall-Olkin Nadarajah-Haghighi (MONH( $\alpha, \theta, \sigma$ )) by Lemonte et al. [28], Marshall-Olkin alpha power exponential (MOAPE( $\alpha, \theta, \sigma$ )) by Nassar et al. [29], alpha power exponential (APE( $\theta, \sigma$ )) by Mahdavi et al. [30], generalized-exponential (GE( $\theta, \sigma$ )) by Gupta et al. [31], Nadarajah-Haghighi (NH( $\theta, \sigma$ )) by Nadarajah et al. [32], Weibull (W( $\theta, \sigma$ )) by Weibull [33], gamma (G( $\theta, \sigma$ )) and exponential (E( $\sigma$ )) by Johnson et al. [34], Lindley (L( $\sigma$ )) by Lindley [35] distributions.

Different goodness-of-fit metrics, including the negative log-likelihood (NL), Akaike information criterion (AIC), Bayesian information criterion (BIC), Hannan-Quinn (HQ), Consistent Akaike (CA), and Kolmogorov-Smirnov (KS) statistic with its  $p$ -value, must be taken into account when comparing two (or more) distributions. The given goodness criteria are computed using the maximum likelihood and its standard-error (St.E) of each unknown parameter, as shown in [Table 2](#). It is evident that the MOL distribution offers a better fit than other rival distributions based on the lowest values of NL, AIC, BIC, HQ, CA, and KS as well as the greatest  $p$ -value.

We also provided the quantile-quantile (QQ) plot as a graphical demonstration, via R 4.1.2 software, for each considered model, see [Fig. 8](#). It is observed, from [Fig. 8](#), that dots are not too far away from the diagonal line follow the diagonal line. It also supports the same results established in [Table 2](#).

In [Fig. 9](#), via R 4.1.2 software, we provided the histograms with the fitted densities as well as plots of the fitted and empirical RFs. [Fig. 9a](#) shows that the fitted density lines captured the data histograms adequately. [Fig. 9b](#) displays that the fitted reliability line of the proposed model captures the empirical reliability line better than others.

**Table 2:** Summary fit of the competitive distributions under vinyl chloride data

Model	MLE (St.E)			NL	AIC	BIC	HQ	CA	KS(P-value)
	$\alpha$	$\theta$	$\sigma$						
MOL	–	0.3663 (0.3084)	0.5464 (0.2305)	55.2866	114.5732	117.6259	115.6143	114.9603	0.0800 (0.9816)
MOE	–	0.8103 (0.4731)	0.4789 (0.1721)	55.3962	114.7924	117.8451	115.8334	115.1795	0.0891 (0.9502)
MOW	1.3260 (0.3429)	0.2584 (0.3974)	0.1780 (0.2340)	55.8635	115.7269	120.3060	117.2885	116.5269	0.0849 (0.9669)
MOG	0.0377 (0.0995)	0.0615 (0.1568)	0.3689 (0.2777)	55.2922	116.2584	120.8375	117.8200	117.0584	0.0928 (0.9316)
MOGE	1.3774 (0.4001)	0.3799 (0.4775)	0.4097 (0.2202)	55.8798	115.7597	120.3387	117.3213	116.5597	0.0840 (0.9701)
MOLE	1.2394 (0.2987)	0.3653 (0.5681)	0.3051 (0.2577)	55.2965	116.1179	120.6970	117.6795	116.9179	0.0805 (0.9802)
MONH	0.2611 (0.3135)	0.0026 (0.0007)	0.0088 (0.0102)	59.8893	125.7786	130.3577	127.3402	126.5786	0.1457 (0.4655)
MOAPE	5.1277 (20.023)	0.3257 (0.8441)	0.4509 (0.2307)	55.3691	116.7382	121.3173	118.2998	117.5382	0.0817 (0.9770)
APE	–	0.6520 (0.8536)	0.4767 (0.1886)	55.3925	114.7850	117.8377	115.8260	115.1721	0.0880 (0.9549)
GE	–	1.0764 (0.2474)	0.5580 (0.1242)	55.4019	114.8037	117.8565	115.8448	115.1908	0.0978 (0.9012)
NH	–	0.9003 (0.3442)	0.6320 (0.4160)	55.4172	114.8345	117.8872	115.8755	115.2216	0.0838 (0.9707)
W	–	1.0102 (0.1327)	1.8879 (0.3390)	55.4496	114.8992	117.9520	115.9403	115.2863	0.0918 (0.9366)
G	–	1.0659 (0.2291)	1.7640 (0.4795)	55.4133	114.8265	117.8793	115.8676	115.2136	0.0979 (0.9001)
L	–	–	0.8238 (0.1054)	56.3036	114.6073	118.1336	115.7807	115.7323	0.1326 (0.5883)
E	–	–	0.5321 (0.0912)	55.4526	115.9052	117.9431	116.4257	116.0302	0.0889 (0.9507)

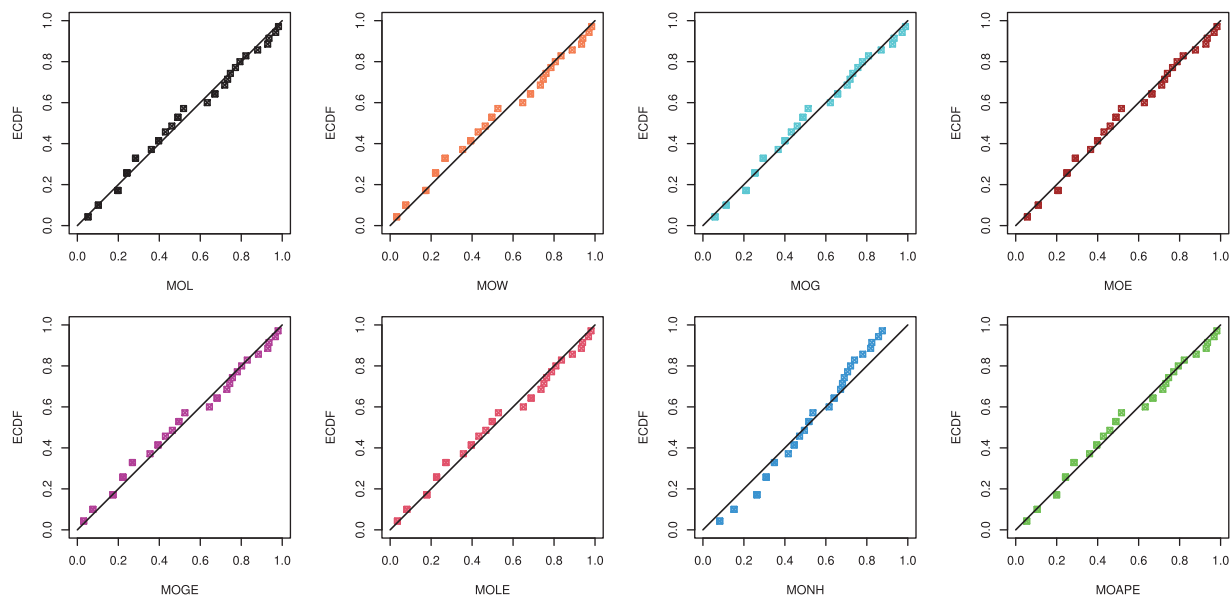


**Figure 8:** The Q-Q plots of the MOL and some competing distributions from vinyl chloride data

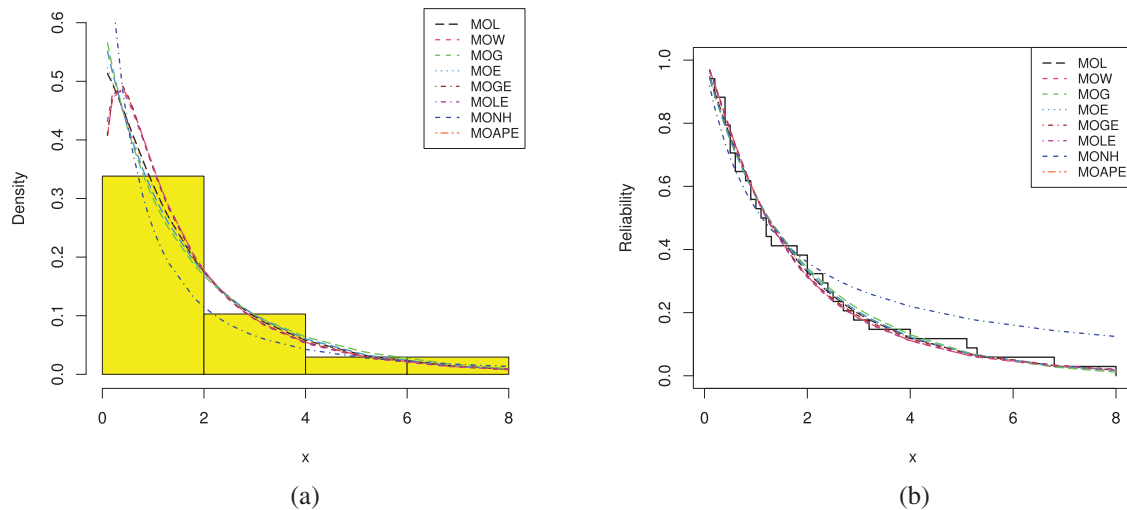


**Figure 9:** (a) Histograms and fitted PDFs and (b) Empirical and fitted RFs under vinyl chloride data

Now three different PT-IIC samples, from the complete vinyl chloride data, are generated with  $m = 20$  based on different schemes and reported in Table 3. From Table 3, the MLEs with their St.Es of  $\theta$ ,  $\sigma$ ,  $R(t)$  and  $h(t)$  (at time  $t = 0.2$ ) are computed. via the M-H algorithm, from 50,000 MCMC samples with 10,000 burn-in, the Bayesian estimates with their St.Es under SE and GENT (for  $\mu(= -3, -0.03, +3)$ ) loss functions of  $\theta$ ,  $\sigma$ ,  $R(t)$  and  $h(t)$  (at  $t = 0.2$ ) are calculated using the improper priors, see Table 4. Also, in Table 5, the two bounds of the 95% ACI/HPD credible interval estimates with their lengths of the unknown parameters are also calculated. The classical estimates of  $\theta$  and  $\sigma$  are selected as the start guesses to apply the proposed MCMC sampler. Before proceeding to calculate the Bayes objectives, we calculate the acceptance rate of Metropolis-Hastings proposals for all created samples, obtained by  $(14, 0^{*}19)$ ,  $(0^{*}9, 7, 7, 0^{*}9)$ , and  $(0^{*}19, 14)$  are: 60.294%, 57.774%, and 60.702%, respectively. It is observed that each MCMC sample gives an acceptable approximation for the posterior density, thus the derived inferences are reliable.

**Table 3:** Three PT-IIC samples from vinyl chloride data

<b>R</b>	<b>Censored sample</b>									
$(14, 0^{*}19)$	0.1	0.2	0.4	0.4	0.4	0.5	0.5	0.6	0.6	0.9
	1.0	1.8	2.0	2.0	2.7	2.9	4.0	5.1	5.3	6.8
$(0^{*}9, 7, 7, 0^{*}9)$	0.1	0.1	0.2	0.2	0.4	0.4	0.4	0.5	0.5	0.5
	0.6	0.8	0.9	1.1	1.2	1.8	2.0	2.7	3.2	5.3
$(0^{*}19, 14)$	0.1	0.1	0.2	0.2	0.4	0.4	0.4	0.5	0.5	0.5
	0.6	0.6	0.8	0.9	0.9	1.0	1.1	1.2	1.2	1.3

From each sample in Table 3, useful statistics for the MCMC variates of  $\theta$ ,  $\sigma$ ,  $R(0.2)$  and  $h(0.2)$  after bun-in, namely: mean, mode, standard deviation (St.D), skewness and quartiles ( $Q_1, Q_2, Q_3$ ) are computed and presented in Table 6. To show the convergence of MCMC variates, based on the sample obtained from  $(14, 0^{*}19)$  (as an example), MCMC trace plots of  $\theta$ ,  $\sigma$ ,  $R(t)$  and  $h(t)$  are displayed in Fig. 10. Using the fitted Gaussian kernel for the sample obtained from  $(14, 0^{*}19)$ , the associated

histograms of the simulated MCMC variates of  $\theta$ ,  $\sigma$ ,  $R(t)$  and  $h(t)$  are also displayed in Fig. 10. All plots shown in Fig. 10 are developed via R 4.1.2 software.

**Table 4:** Point estimates (first-column) with their St.Es (second-column) of  $\theta$ ,  $\sigma$ ,  $R(t)$  and  $h(t)$  from vinyl chloride data

R	Par.	ML		SE		GEnt					
		$\mu \rightarrow$						-3	-0.03	+3	
(14, 0*19)	$\theta$	0.3922	0.4045	0.3604	0.0578	0.3668	0.0254	0.3572	0.0350	0.3468	0.0455
	$\sigma$	0.5459	0.2801	0.5182	0.0532	0.5222	0.0238	0.5163	0.0297	0.5101	0.0359
	$R(0.2)$	0.9037	0.0344	0.9026	0.0162	0.9028	0.0009	0.9024	0.0013	0.9020	0.0017
	$h(0.2)$	0.0900	0.1594	0.0768	0.0207	0.0801	0.0099	0.0752	0.0148	0.0700	0.0201
(0*9, 7, 7, 0*9)	$\theta$	0.8223	0.7626	0.7077	0.1474	0.7197	0.1026	0.7017	0.1205	0.6828	0.1394
	$\sigma$	0.9355	0.4463	0.8395	0.1279	0.8479	0.0876	0.8353	0.1002	0.8223	0.1132
	$R(0.2)$	0.8921	0.0337	0.8928	0.0177	0.8931	0.0010	0.8926	0.0005	0.8921	0.0001
	$h(0.2)$	0.4148	0.6293	0.3097	0.1240	0.3234	0.0914	0.3029	0.1119	0.2816	0.1332
(0*19, 14)	$\theta$	2.2517	2.6453	2.1375	0.1532	2.1424	0.1093	2.1351	0.1166	2.1277	0.1240
	$\sigma$	1.5514	0.8284	1.4534	0.1349	1.4593	0.0922	1.4505	0.1009	1.4414	0.1101
	$R(0.2)$	0.9125	0.0360	0.9160	0.0087	0.9160	0.0035	0.9159	0.0034	0.9158	0.0033
	$h(0.2)$	2.0483	3.4938	1.8029	0.2983	1.8188	0.2295	1.7951	0.2532	1.7700	0.2783

**Table 5:** Interval estimates of  $\theta$ ,  $\sigma$ ,  $R(t)$  and  $h(t)$  from vinyl chloride data

R	Par.	ACI			HPD		
		Lower	Upper	Length	Lower	Upper	Length
(14, 0*19)	$\theta$	0.0000	1.1850	1.1850	0.2725	0.4616	0.1891
	$\sigma$	0.0000	1.0950	1.0950	0.4282	0.6060	0.1778
	$R(0.2)$	0.8363	0.9711	0.1348	0.8699	0.9315	0.0616
	$h(0.2)$	0.0000	0.4025	0.4025	0.0462	0.1071	0.0609
(0*9, 7, 7, 0*9)	$\theta$	0.0000	2.3169	2.3169	0.5426	0.8979	0.3553
	$\sigma$	0.0608	1.8102	1.7494	0.6803	0.9998	0.3195
	$R(0.2)$	0.8260	0.9582	0.1322	0.8571	0.9253	0.0682
	$h(0.2)$	0.0000	1.6482	1.6482	0.1758	0.4279	0.2521
(0*19, 14)	$\theta$	0.0000	7.4364	7.4364	1.9168	2.3167	0.3999
	$\sigma$	0.0000	3.1750	3.1750	1.2772	1.6278	0.3506
	$R(0.2)$	0.8419	0.9831	0.1411	0.9000	0.9306	0.0307
	$h(0.2)$	0.0000	8.8960	8.8960	1.4757	2.1203	0.6447

**Table 6:** Some statistics for MCMC draws of  $\theta$ ,  $\sigma$ ,  $R(t)$  and  $h(t)$  from vinyl chloride data

<b>R</b>	Par.	Mean	Mode	St.D	Skewness	$Q_1$	$Q_2$	$Q_3$
(14, 0*19)	$\theta$	0.36042	0.26397	0.04829	0.03778	0.32680	0.36034	0.39294
	$\sigma$	0.51820	0.37151	0.04542	0.04602	0.48720	0.51779	0.54846
	$R(0.2)$	0.90255	0.92379	0.01614	-0.47811	0.89248	0.90385	0.91391
	$h(0.2)$	0.07685	0.03204	0.01596	0.33424	0.06552	0.07587	0.08718
(0*9, 7, 7, 0*9)	$\theta$	0.70765	0.51841	0.09269	0.14656	0.64118	0.70368	0.77130
	$\sigma$	0.83947	0.68510	0.08437	0.13151	0.78220	0.83775	0.89489
	$R(0.2)$	0.89277	0.89141	0.01774	-0.45987	0.88186	0.89432	0.90495
	$h(0.2)$	0.30968	0.17580	0.06571	0.37362	0.26288	0.30679	0.35120
(0*19, 14)	$\theta$	2.13750	1.91678	0.10214	0.00815	2.06689	2.13791	2.20741
	$\sigma$	1.45340	1.34267	0.09263	-0.02278	1.38835	1.45304	1.51779
	$R(0.2)$	0.91595	0.91698	0.00795	-0.13721	0.91065	0.91639	0.92125
	$h(0.2)$	1.80292	1.47569	0.16970	0.01186	1.68844	1.80353	1.91608

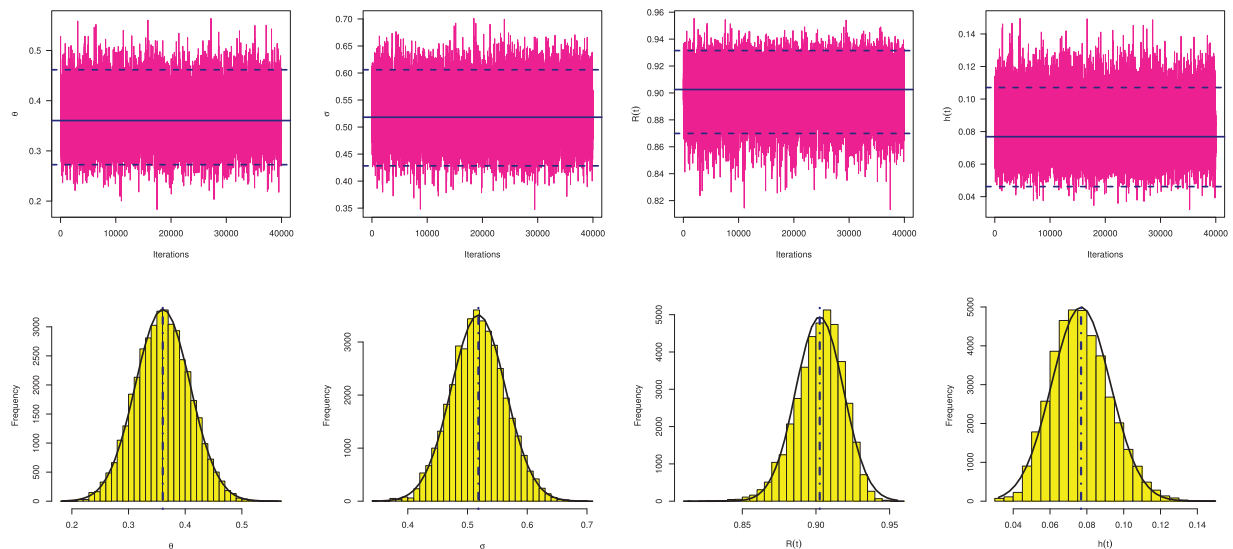


**Figure 10:** Trace (top) and Histograms (bottom) plots of  $\theta$ ,  $\sigma$ ,  $R(t)$  and  $h(t)$  from vinyl chloride data

In each trace plot, the sample mean and two bounds of 95% HPD credible intervals of  $\theta$ ,  $\sigma$ ,  $R(t)$  or  $h(t)$  are represented with solid- and dashed-horizontal lines, respectively. Additionally, each sample mean of  $\theta$ ,  $\sigma$ ,  $R(t)$  or  $h(t)$  is represented with vertical dotted (:) line. Fig. 10 shows that the MCMC sampler converges quite well and indicates the burn-in sample has an appropriate size to eliminate the effect of the initial values. It is also observed, from Fig. 10, that the generated MCMC variates of  $\theta$  and  $\sigma$  are fairly symmetrical while of  $R(t)$  and  $h(t)$  are negative and positive quite skewed, respectively. For brevity, other trace and histogram plots of  $\theta$ ,  $\sigma$ ,  $R(t)$  and  $h(t)$  based on the PT-IIC samples obtained from (0\*9, 7, 7, 0\*9) and (0\*19, 14) are plotted and reported in the supplementary file.

### 5.2 Mechanical Equipments

In this application, from the engineering field, we will explain our theoretical results based on the time between consecutive failures for repairable mechanical equipment (RME) items depicted in Table 7. Murthy et al. [36] initially conveyed this data and it has also been examined by Elshahhat et al. [37], Nassar et al. [38], and Elshahhat et al. [39]. Employing the competitive statistical distributions as well as the model selection criteria proposed in Subsection 5.1, the MOL distribution based on the complete RME data is compared. All results of the MOL distribution and other models are provided in Table 8. It suggests that the MOL distribution is the most suitable model to fit the MRE data when compared to others.

**Table 7:** Failure times of 30 repairable mechanical equipments

0.11	0.30	0.40	0.45	0.59	0.63	0.70	0.71	0.74	0.77
0.94	1.06	1.17	1.23	1.23	1.24	1.43	1.46	1.49	1.74
1.82	1.86	1.97	2.23	2.37	2.46	2.63	3.46	4.36	4.73

**Table 8:** Summary fit of the competitive distributions under RME data

Model	MLE(SE)			NL	AIC	BIC	HQ	CA	KS( <i>p</i> -value)
	$\alpha$	$\theta$	$\sigma$						
MOL	–	2.7991 (1.8462)	1.4400 (0.3462)	40.4944	84.9887	85.8852	87.7911	85.4331	0.0746 (0.9962)
MOE	–	5.1690 (3.7002)	1.3178 (0.3523)	40.5040	85.0081	85.9046	87.8105	85.4525	0.0910 (0.9648)
MOW	1.9211 (0.6269)	0.2424 (0.4112)	0.1467 (0.2446)	40.5347	85.0694	86.4141	89.2730	85.9924	0.0752 (0.9958)
MOG	2.1276 (1.3850)	10.314 (13.352)	0.2181 (0.2838)	40.5645	86.3289	87.6737	90.5325	87.2520	0.0790 (0.9920)
MOGE	2.1159 (1.5457)	0.9994 (2.9184)	0.9765 (0.7803)	40.6319	85.2638	86.6086	89.4674	86.1869	0.0748 (0.9960)
MOLE	1.2345 (0.7252)	3.5295 (12.180)	0.9511 (1.4986)	40.5666	86.1333	87.4780	90.3369	87.0564	0.0977 (0.9371)
MONH	0.9138 (0.2353)	4.4984 (3.4947)	1.4696 (1.0112)	40.5187	86.8373	88.1821	91.0409	87.7604	0.0791 (0.9920)
MOAPE	0.0446 (0.2008)	12.908 (16.559)	0.9549 (0.7361)	41.0248	86.0495	87.3943	90.2531	86.9726	0.0750 (0.9959)
APE	–	9.9305 (8.4422)	1.0697 (0.1976)	40.5782	85.0356	86.0253	87.8589	85.8009	0.0826 (0.9867)
GE	–	2.1234 (0.5875)	1.0032 (0.2014)	40.6143	85.2287	86.0125	87.8031	85.6731	0.0750 (0.9958)
NH	–	4.4288 (6.6965)	0.0981 (0.1699)	41.1540	86.3080	87.2045	89.1103	86.7524	0.1132 (0.8365)
W	–	1.4663 (0.2032)	1.7103 (0.2250)	40.9105	85.0821	86.0717	87.8623	85.6543	0.0751 (0.9958)
G	–	1.9718 (0.4717)	0.7820 (0.2127)	40.6296	85.0259	86.1558	88.0617	85.7037	0.0769 (0.9929)
L	–	–	0.9762 (0.1345)	41.5473	85.0946	86.0543	87.9576	85.7416	0.1407 (0.5928)
E	–	–	0.6482 (0.1184)	43.0054	88.0108	88.4590	89.4119	88.1536	0.1845 (0.2589)

Also, using the complete RME data, Fig. 11 displays the QQ plots of MOL, MOE, MOW, MOG, MOGE, MOLE, MONH and MOAPE distributions. It supports the same findings reported in Table 8 also. Further, three graphics of goodness-of-fit are investigated; (i) plot of histograms of RME data with fitted PDFs, and (ii) plot of the fitted and empirical RFs under RME data are shown in Fig. 12. It indicates that the MOL distribution is the best model compared to its competitive models.

From the complete RME data, three different PT-IIC samples are generated with  $m = 10$  based on different schemes and provided in Table 9. From each generated sample in Table 9, the maximum likelihood and Bayesian estimates with their St.Es of  $\theta$ ,  $\sigma$ ,  $R(t)$  and  $h(t)$  (at time  $t = 0.5$ ) are computed and presented in Table 10. Two-sided 95% ACI and HPD credible interval estimates with their lengths of  $\theta$ ,  $\sigma$ ,  $R(t)$  and  $h(t)$  are also calculated and reported in Table 11. Via improper priors, utilizing 50,000

MCMC draws with 10,000 burn-in, the Bayesian analysis is performed based on both SE and GEnt (for  $\mu (= -5, -0.05, +5)$ ) (Table 12). Using the PT-IIC samples generated by  $(20, 0^*9)$ ,  $(0^*4, 10, 10, 0^*4)$  and  $(0^*9, 20)$ , the acceptance rates of the Metropolis-Hastings proposals are 61.824%, 61.132%, and 61.154%, respectively. These rates support the same result reported in Application 5.1, which is that the percentage of iterations in which the proposals were accepted is much higher.

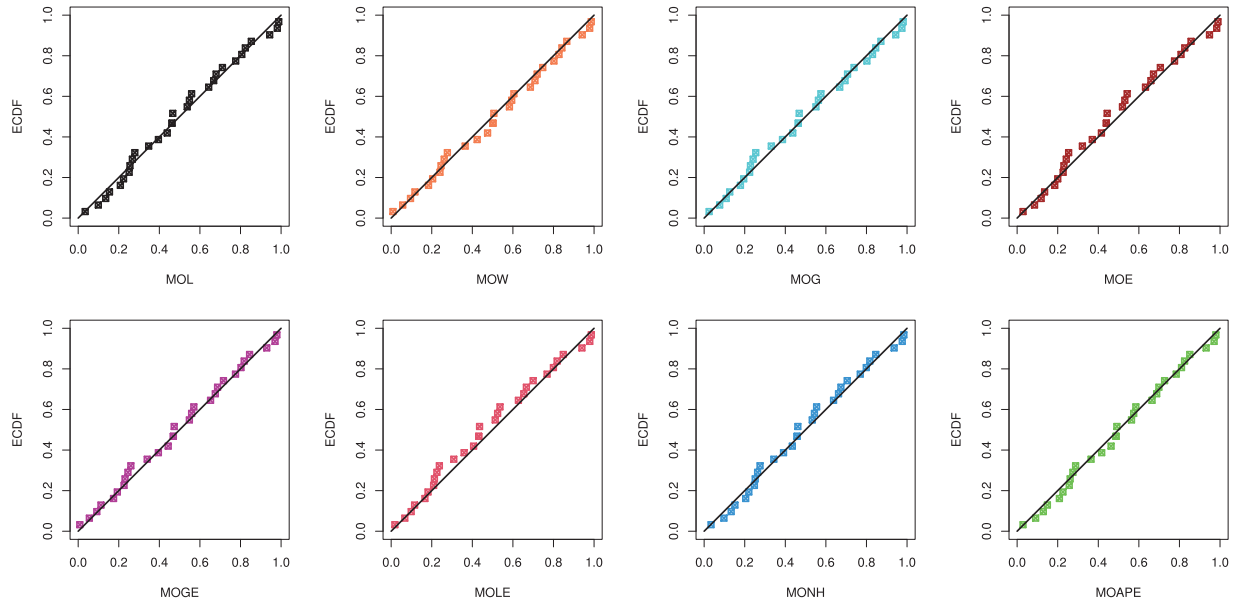


**Figure 11:** The Q-Q plots of the competing models from mechanical equipments data

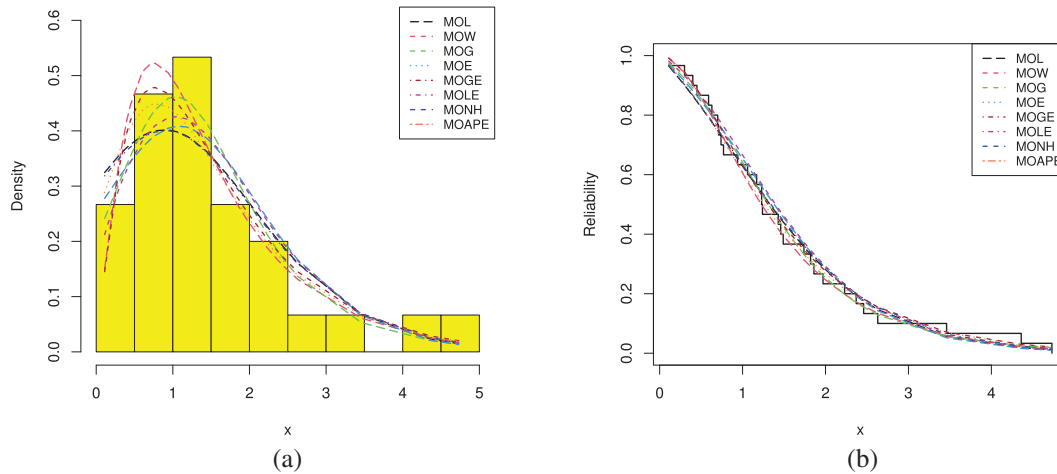


**Figure 12:** (a) Histograms and fitted PDFs and (b) Empirical and fitted RFs from the RME data

From the PT-IIC sample generated by  $(20, 0^*9)$ , trace and histogram plots of the MCMC simulated variates of all unknown parameters are provided in Fig. 13. It shows that the MCMC mechanism converges well and demonstrates that the MCMC variates of  $\theta$ ,  $\sigma$ ,  $R(t)$  and  $h(t)$  are fairly symmetrical. Other plots of  $\theta$ ,  $\sigma$ ,  $R(t)$  and  $h(t)$  based on  $(0^*4, 10, 10, 0^*4)$  and  $(0^*9, 20)$  are available in the supplementary file. Lastly, from both chemical and engineering examples, one can decide that

the results of the proposed methodologies provide a good explanation to the proposed MOL lifetime model.

**Table 9:** Three PT-IIC samples from RME data

<b>R</b>	<b>Censored sample</b>									
(20, 0*9)	0.11	0.59	0.63	0.70	0.71	0.77	1.06	1.23	1.46	2.46
(0*4, 10, 10, 0*4)	0.11	0.40	0.59	0.74	0.77	0.94	1.23	1.74	1.86	2.63
(0*9, 20)	0.11	0.30	0.40	0.45	0.59	0.63	0.70	0.71	0.74	0.77

**Table 10:** Point estimates (first-column) with their St.Es (second-column) of  $\theta$ ,  $\sigma$ ,  $R(t)$  and  $h(t)$  from RME data

<b>R</b>	Par.	ML	SE		GEnt						
					$\mu \rightarrow$		-5		-0.05		+5
(20, 0*9)	$\theta$	10.649	10.654	10.547	0.1423	10.549	0.0994	10.547	0.1018	10.544	0.1042
	$\sigma$	3.2107	1.0042	3.1126	0.1369	3.1185	0.0922	3.1112	0.0995	3.1039	0.1069
	$R(0.5)$	0.8034	0.0849	0.8120	0.0131	0.8123	0.0088	0.8120	0.0085	0.8116	0.0082
	$h(0.5)$	9.7741	7.9925	9.6747	0.1266	9.6760	0.0982	9.6744	0.0997	9.6728	0.1013
(0*4, 10, 10, 0*4)	$\theta$	22.117	8.9012	22.021	0.1350	22.022	0.0947	22.021	0.0957	22.020	0.0967
	$\sigma$	2.5831	0.4318	2.4900	0.1333	2.4973	0.0858	2.4883	0.0948	2.4790	0.1041
	$R(0.5)$	0.9296	0.0207	0.9338	0.0062	0.9338	0.0042	0.9338	0.0041	0.9337	0.0041
	$h(0.5)$	18.265	7.0823	18.076	0.2345	18.079	0.1864	18.076	0.1890	18.073	0.1918
(0*9, 20)	$\theta$	58.181	17.183	58.080	0.1420	58.081	0.1002	58.080	0.1007	58.080	0.1011
	$\sigma$	5.0245	0.6102	4.9259	0.1396	4.9299	0.0946	4.9250	0.0995	4.9199	0.1045
	$R(0.5)$	0.8831	0.0294	0.8883	0.0076	0.8884	0.0053	0.8883	0.0052	0.8882	0.0052
	$h(0.5)$	33.580	7.0719	34.205	0.9234	34.232	0.6516	34.199	0.6181	34.164	0.5840

**Table 11:** Interval estimates of  $\theta$ ,  $\sigma$ ,  $R(t)$  and  $h(t)$  from RME data

<b>R</b>	Par.	ACI			HPD		
		Lower	Upper	Length	Lower	Upper	Length
(20, 0*9)	$\theta$	0.0000	31.530	31.530	10.346	10.741	0.3948
	$\sigma$	1.2424	5.1790	3.9366	2.9245	3.2943	0.3697
	$R(0.5)$	0.6371	0.9697	0.3326	0.7923	0.8306	0.0383
	$h(0.5)$	0.0000	25.439	25.439	9.5034	9.8159	0.3125
(0*4, 10, 10, 0*4)	$\theta$	4.6708	39.563	34.892	21.841	22.215	0.3738
	$\sigma$	1.7368	3.4293	1.6925	2.3026	2.6754	0.3728
	$R(0.5)$	0.8890	0.9703	0.0813	0.9247	0.9425	0.0178
	$h(0.5)$	4.3840	32.146	27.762	17.789	18.324	0.5344
(0*9, 20)	$\theta$	24.503	91.859	67.356	57.898	58.280	0.3819
	$\sigma$	3.8285	6.2204	2.3919	4.7400	5.1153	0.3752

(Continued)

**Table 11 (continued)**

R	Par.	ACI			HPD		
		Lower	Upper	Length	Lower	Upper	Length
	$R(0.5)$	0.8255	0.9407	0.1151	0.8775	0.8982	0.0207
	$h(0.5)$	19.720	47.441	27.721	32.862	35.460	2.5979

**Table 12:** Some statistics for MCMC draws of  $\theta$ ,  $\sigma$ ,  $R(t)$  and  $h(t)$  from RME data

R	Par.	Mean	Mode	St.D	Skewness	$Q_1$	$Q_2$	$Q_3$
(20, 0*9)	$\theta$	10.5473	10.2897	0.09996	0.01633	10.4822	10.5465	10.6134
	$\sigma$	3.11263	3.09570	0.09553	0.09140	3.04572	3.11020	3.17706
	$R(0.5)$	0.81202	0.81011	0.00995	-0.14604	0.80544	0.81218	0.81902
	$h(0.5)$	9.67470	9.48238	0.07831	-0.00812	9.62314	9.67474	9.72670
(0*4, 10, 10, 0*4)	$\theta$	22.0214	21.8156	0.09544	0.13513	21.9559	22.0168	22.0847
	$\sigma$	2.49003	2.39730	0.09541	-0.02557	2.42499	2.49036	2.55517
	$R(0.5)$	0.93376	0.93764	0.00456	-0.08578	0.93070	0.93382	0.93693
	$h(0.5)$	18.0765	17.8060	0.13949	-0.43657	17.9895	18.0877	18.1746
(0*9, 20)	$\theta$	58.0804	57.9260	0.10016	0.00309	58.0092	58.0809	58.1483
	$\sigma$	4.92592	4.75752	0.09890	-0.03977	4.85957	4.92677	4.99215
	$R(0.5)$	0.88834	0.89721	0.00546	-0.07519	0.88471	0.88844	0.89206
	$h(0.5)$	34.2049	35.2789	0.68016	0.06226	33.7409	34.1986	34.6577

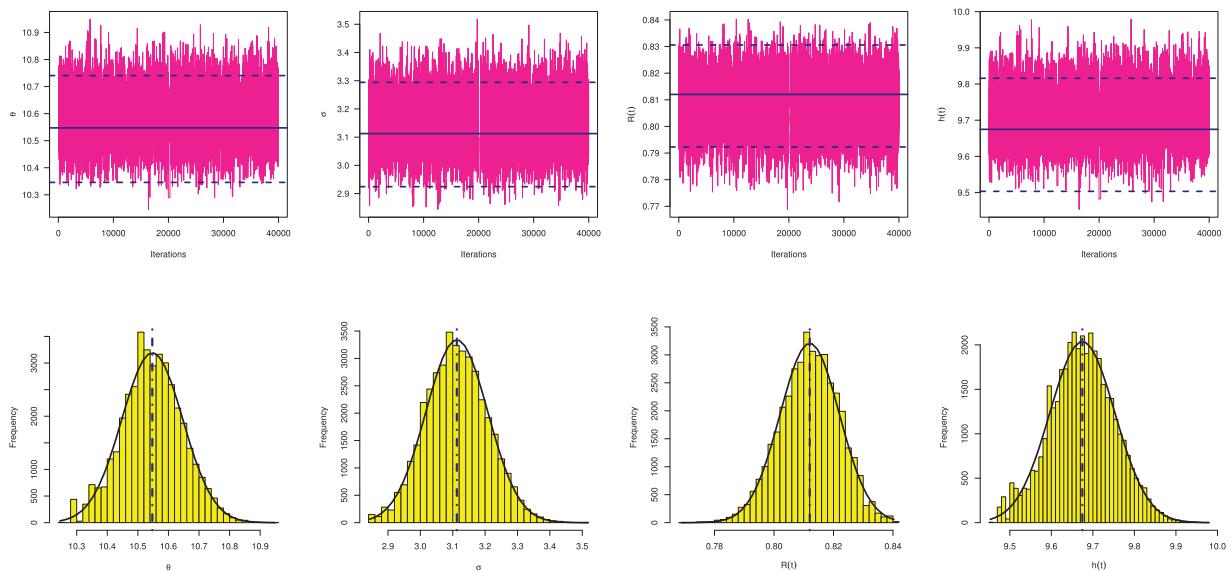


**Figure 13:** Trace (top) and Histograms (bottom) plots of  $\theta$ ,  $\sigma$ ,  $R(t)$  and  $h(t)$  from RME data

## 6 Concluding Remarks

In this study, we looked into the statistical inference of the Marshall-Olkin Lindley distribution's unknown parameters, reliability, and hazard rate functions under progressively Type-II censored data. The various parameters of interest are inferred using both classical and Bayesian methods. The normal approximation of the maximum likelihood estimators is also used to create the approximate confidence intervals. The Bayesian estimations are addressed by employing independent gamma priors and symmetric and asymmetric loss functions. We have indicated that the explicit expressions of the proposed Bayesian estimators are not available. The Markov Chain Monte Carlo technique is employed as a result. For each parameter, the highest posterior density credible intervals are also attained. We conducted a thorough simulation analysis and examined two applications to real-world data sets to evaluate the effectiveness of the delivered estimations. The findings of the numerical study showed that when progressively Type-II censored data were given, the suggested point and interval estimations of the Marshall-Olkin Lindley distribution acted reasonably. More specifically, the highest posterior density credible intervals were advised and the Bayesian estimates utilizing the general entropy loss function outperformed all other estimates. In addition, the real data analysis showed that the Marshall-Olkin Lindley distribution could be used as a good model to fit vinyl chloride and repairable mechanical equipment data sets rather than some other Marshall-Olkin models, including Marshall-Olkin Weibull, Marshall-Olkin Gompertz, Marshall-Olkin generalized exponential and Marshall-Olkin logistic-exponential distributions. In future work, it is of interest to investigate the estimation problems of the considered distribution based on other censoring schemes like an adaptive progressive Type-II censoring scheme. Another significant future work to be addressed is exploring the performance of dependability metrics of the utilized model in the case of accelerated life tests.

**Acknowledgement:** The authors would desire to express their thanks to the editor and the three anonymous referees for useful suggestions and valuable comments. Princess Nourah bint Abdulrahman University Researchers Supporting Project and Princess Nourah bint Abdulrahman University, Riyadh, Saudi Arabia.

**Funding Statement:** This research was funded by Princess Nourah bint Abdulrahman University Researchers Supporting Project Number (PNURSP2023R50), Princess Nourah bint Abdulrahman University, Riyadh, Saudi Arabia.

**Author Contributions:** The authors confirm contribution to the paper as follows: study conception and design: R. Alotaibi, M. Nassar, and A. Elshahhat; data collection: A. Elshahhat; analysis and interpretation of results: A. Elshahhat; draft manuscript preparation: M. Nassar, R. Alotaibi. All authors reviewed the results and approved the final version of the manuscript.

**Availability of Data and Materials:** The data that support the findings of this study are available in the text.

**Conflicts of Interest:** The authors declare that they have no conflicts of interest to report regarding the present study.

**Supplementary Materials:** The supplementary material is available online at <https://doi.org/10.32604/cmcs.2023.030582>.

## References

1. Ghitany, M. E., Al-Mutairi, D. K., Al-Awadhi, F. A., Al-Burais, M. M. (2012). Marshall-Olkin extended Lindley distribution and its application. *International Journal of Applied Mathematics*, 25(5), 709–721.
2. do Espirito Santo, A. P. J., Mazucheli, J. (2015). Comparison of estimation methods for the Marshall-Olkin extended Lindley distribution. *Journal of Statistical Computation and Simulation*, 85(17), 3437–3450.
3. Balakrishnan, N., Aggarwala, R. (2000). *Progressive censoring: Theory, methods, and applications*. Birkhäuser, Boston: Springer Science & Business Media.
4. Balakrishnan, N., Cramer, E. (2014). *The art of progressive censoring*. Birkhäuser, New York: Springer.
5. Sultan, K. S., Alsadat, N. H., Kundu, D. (2014). Bayesian and maximum likelihood estimations of the inverse Weibull parameters under progressive type-II censoring. *Journal of Statistical Computation and Simulation*, 84(10), 2248–2265.
6. Guo, L., Gui, W. (2018). Statistical inference of the reliability for generalized exponential distribution under progressive type-II censoring schemes. *IEEE Transactions on Reliability*, 67(2), 470–480.
7. Joukar, A., Ramezani, M., MirMostafaei, S. M. T. K. (2020). Estimation of  $P(X > Y)$  for the power Lindley distribution based on progressively type II right censored samples. *Journal of Statistical Computation and Simulation*, 90(2), 355–389.
8. Elshahhat, A., Rastogi, M. K. (2021). Estimation of parameters of life for an inverted Nadarajah-Haghighi distribution from Type-II progressively censored samples. *Journal of the Indian Society for Probability and Statistics*, 22(1), 113–154.
9. Alotaibi, R., Nassar, M., Rezk, H., Elshahhat, A. (2022). Inferences and engineering applications of alpha power Weibull distribution using progressive Type-II censoring. *Mathematics*, 10(16), 2901.
10. Okasha, H., Nassar, M. (2022). Product of spacing estimation of entropy for inverse Weibull distribution under progressive type-II censored data with applications. *Journal of Taibah University for Science*, 16(1), 259–269.
11. Maiti, K., Kayal, S., Kundu, D. (2022). Statistical Inference on the shannon and rényi entropy measures of generalized exponential distribution under the progressive censoring. *SN Computer Science*, 3(4), 1–21.
12. Calabria, R., Pulcini, G. (1994). An engineering approach to Bayes estimation for the Weibull distribution. *Microelectronics Reliability*, 34(5), 789–802.
13. Henningsen, A., Toomet, O. (2011). maxLik: A package for maximum likelihood estimation in R. *Computational Statistics*, 26(3), 443–458.
14. Kundu, D. (2008). Bayesian inference and life testing plan for the Weibull distribution in presence of progressive censoring. *Technometrics*, 50(2), 144–154.
15. Dey, S., Elshahhat, A., Nassar, M. (2022). Analysis of progressive type-II censored gamma distribution. *Computational Statistics*, 38(1), 481–508.
16. Plummer, M., Best, N., Cowles, K., Vines, K. (2006). CODA: Convergence diagnosis and output analysis for MCMC. *R News*, 6, 7–11.
17. Roy, V. (2020). Convergence diagnostics for Markov Chain Monte Carlo. *Annual Review of Statistics and Its Application*, 7(1), 387–412.
18. Elshahhat, A. (2022). R programming language for data analytics. *The 55th Annual International Conference on Data Science*, Egypt, Cairo University. <https://doi.org/10.13140/RG.2.2.15044.09607/1>
19. Bhaumik, D. K., Kapur, K., Gibbons, R. D. (2009). Testing parameters of a gamma distribution for small samples. *Technometrics*, 51(3), 326–334.
20. Elshahhat, A., Elemetry, B. R. (2021). Analysis for xgamma parameters of life under type-II adaptive progressively hybrid censoring with applications in engineering and chemistry. *Symmetry*, 13(11), 2112.
21. Alotaibi, R., Nassar, M., Elshahhat, A. (2022). Computational analysis of XLindley parameters using adaptive Type-II progressive hybrid censoring with applications in chemical engineering. *Mathematics*, 10(18), 3355.

22. Elshahhat, A., Dutta, S., Abo-Kasem, O. E., Mohammed, H. S. (2023). Statistical analysis of the Gompertz-Makeham model using adaptive progressively hybrid Type-II censoring and its applications in various sciences. *Journal of Radiation Research and Applied Sciences*, 16(4), 100644. <https://doi.org/10.1016/j.jrras.2023.100644>
23. Marshall, A. W., Olkin, I. (1997). A new method for adding a parameter to a family of distributions with application to the exponential and Weibull families. *Biometrika*, 84(3), 641–652.
24. Cordeiro, G. M., Lemonte, A. J. (2013). On the Marshall-Olkin extended Weibull distribution. *Statistical Papers*, 54(2), 333–353.
25. Eghwerido, J. T., Ogbo, J. O., Omotoye, A. E. (2021). The Marshall-Olkin Gompertz distribution: Properties and applications. *Statistica*, 81, 183–215.
26. Ristić, M. M., Kundu, D. (2015). Marshall-Olkin generalized exponential distribution. *Metron*, 73(3), 317–333.
27. Mansoor, M., Tahir, M. H., Cordeiro, G. M., Provost, S. B., Alzaatreh, A. (2019). The Marshall-Olkin logistic-exponential distribution. *Communications in Statistics-Theory and Methods*, 48(2), 220–234.
28. Lemonte, A. J., Cordeiro, G. M., Moreno-Arenas, G. (2016). A new useful three-parameter extension of the exponential distribution. *Statistics*, 50, 312–337.
29. Nassar, M., Kumar, D., Dey, S., Cordeiro, G. M., Afify, A. Z. (2019). The Marshall-Olkin alpha power family of distributions with applications. *Journal of Computational and Applied Mathematics*, 351, 41–53.
30. Mahdavi, A., Kundu, D. (2017). A new method for generating distributions with an application to exponential distribution. *Communications in Statistics-Theory and Methods*, 46(13), 6543–6557.
31. Gupta, R. D., Kundu, D. (1999). Theory and methods: Generalized exponential distributions. *Australian and New Zealand Journal of Statistics*, 41(2), 173–188.
32. Nadarajah, S., Haghighi, F. (2011). An extension of the exponential distribution. *Statistics*, 45(6), 543–558.
33. Weibull, W. (1951). A statistical distribution function of wide applicability. *Journal of Applied Mechanics*, 18(3), 293–297.
34. Johnson, N., Kotz, S., Balakrishnan, N. (1994). *Continuous univariate distributions*. 2nd edition. New York: John Wiley and Sons.
35. Lindley, D. V. (1958). Fiducial distributions and Bayes' theorem. *Journal of the Royal Statistical Society: Series B*, 20, 102–107.
36. Murthy, D. N. P., Xie, M., Jiang, R. (2004). Weibull models. In: *Wiley series in probability and statistics*. New Jersey: John Wiley and Sons.
37. Elshahhat, A., Aljohani, H. M., Afify, A. Z. (2021). Bayesian and classical inference under Type-II censored samples of the extended inverse gompertz distribution with engineering applications. *Entropy*, 23(12), 1578.
38. Nassar, M., Elshahhat, A. (2023). Estimation procedures and optimal censoring schemes for an improved adaptive progressively type-II censored Weibull distribution. *Journal of Applied Statistics*. <https://doi.org/10.1080/02664763.2023.2230536>
39. Elshahhat, A., Almetwally, E. M., Dey, S., Mohammed, H. S. (2023). Analysis of WE parameters of life using adaptive-progressively Type-II hybrid censored mechanical equipment data. *Axioms*, 12(7), 690.